iScience

CellPress

Article

Tet1 Deficiency Leads to Premature Reproductive Aging by Reducing Spermatogonia Stem Cells and Germ Cell Differentiation

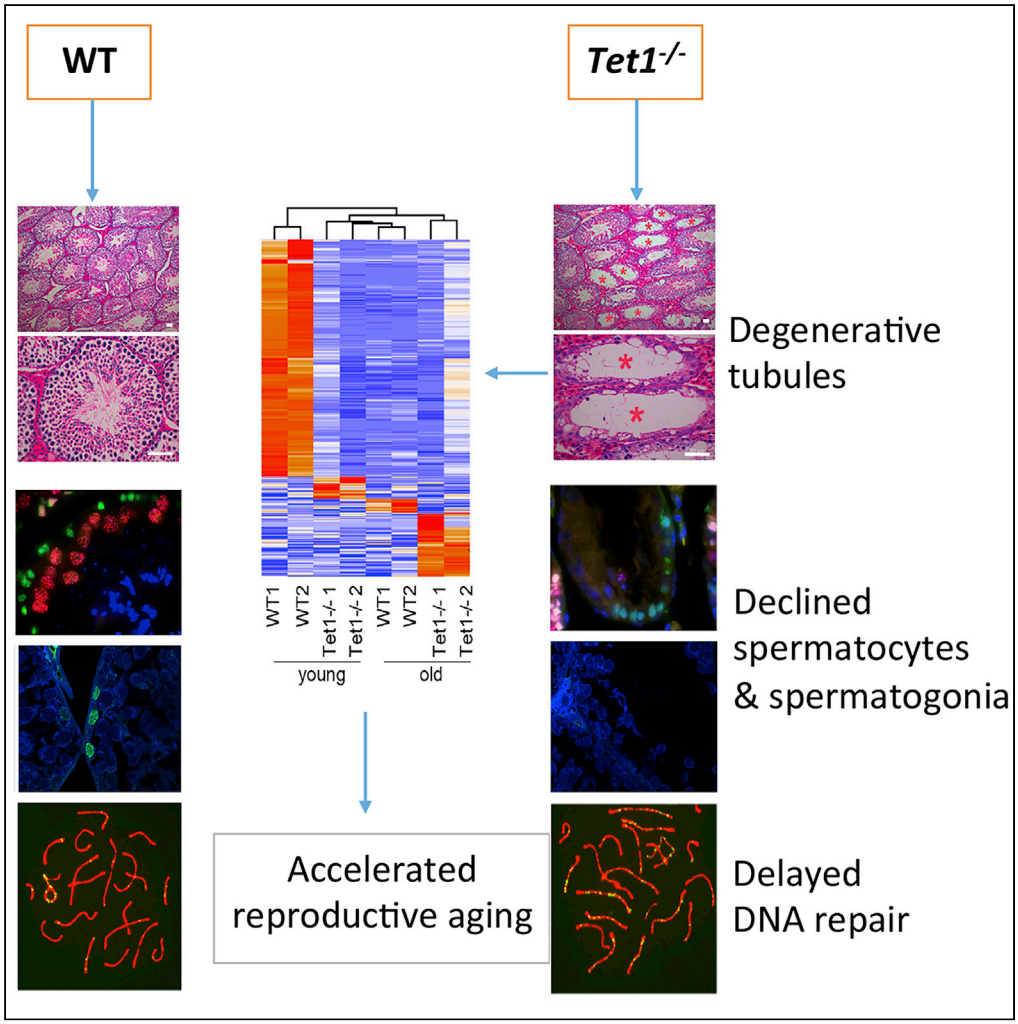

Guian Huang, Linlin Liu, Huasong Wang, ..., Tian-Tian Zhou, Guo-Liang Xu, Lin Liu

glxu@sibcb.ac.cn (G.-L.X.)
liulin@nankai.edu.cn (L.L.)

HIGHLIGHTS

Tet1 regulates stem cell aging and differentiation

Tet1 plays an important role in maintaining spermatogonial stem cells

Loss of Tet1 results in exhaustion of spermatogonia and premature reproductive aging

Effect of Tet2 deficiency on reproductive aging in males is minor

DATA AND CODE AVAILABILITY

GSE140014
GSE140999

Huang et al., iScience *23*, 100908
March 27, 2020
https://doi.org/10.1016/j.isci.2020.100908

iScience

CellPress

Article

Tet1 Deficiency Leads to Premature Reproductive Aging by Reducing Spermatogonia Stem Cells and Germ Cell Differentiation

Guian Huang,[1,2,4] Linlin Liu,[1,2,4] Huasong Wang,[1,2,4] Mo Gou,[1,2] Peng Gong,[1,2] Chenglei Tian,[1,2] Wei Deng,[1,2] Jiao Yang,[1,2] Tian-Tian Zhou,[3] Guo-Liang Xu,[3,*] and Lin Liu[1,2,5,*]

SUMMARY

Ten-eleven translocation (Tet) enzymes are involved in DNA demethylation, important in regulating embryo development, stem cell pluripotency and tumorigenesis. Alterations of DNA methylation with age have been shown in various somatic cell types. We investigated whether Tet1 and Tet2 regulate aging. We showed that *Tet1*-deficient mice undergo a progressive reduction of spermatogonia stem cells and spermatogenesis and thus accelerated infertility with age. *Tet1* deficiency decreases 5hmC levels in spermatogonia and downregulates a subset of genes important for cell cycle, germ cell differentiation, meiosis and reproduction, such as *Ccna1* and *Spo11*, resulting in premature reproductive aging. Moreover, Tet1 and 5hmC both regulate signaling pathways key for stem cell development, including Wnt and PI3K-Akt, autophagy and stress response genes. In contrast, effect of *Tet2* deficiency on male reproductive aging is minor. Hence, Tet1 maintains spermatogonia stem cells with age, revealing an important role of Tet1 in regulating stem cell aging.

INTRODUCTION

Mammalian aging involves many aspects of cellular and molecular changes, such as genomic instability, telomere attrition, epigenetic alterations, stem cell exhaustion etc (Lopez-Otin et al., 2013). Deeper understanding of epigenetic alterations in aging is of particular interest as epigenetic modifications can be reversed, allowing manipulation to potentially reverse aging and thus therapeutic potential (Chen and Kerr, 2019), unlike genomic mutations which are not readily fixable.

As the best studied epigenetic modifications, DNA methylation at the 5-position of cytosine (5-methylcytosine, 5mC) plays essential roles in development, aging and disease (Greenberg and Bourc'his, 2019; Tan and Shi, 2012). DNA methylation changes have become a hallmark of aging (Lopez-Otin et al., 2013). The DNA methylation signature as 'epigenetic clocks' can predict the stage of body aging for any tissue across the entire life course (Horvath, 2013). Most methylation changes occur in a programmed manner in a subpopulation of tissue cells during natural aging, probably predisposing them toward tumorigenesis (Klutstein et al., 2016). Additionally, age-associated methylation perturbations represent a plausible mechanism by which the increased incidence of disease in the offspring of older fathers may be transmitted (Jenkins et al., 2014, 2015).

Cytosine methylation is introduced by DNA methyltransferases such as Dnmt1, Dnmt3a and Dnmt3b. Active DNA demethylation is mainly mediated by Ten-eleven translocation (Tet) enzymes, including Tet1, Tet2, and Tet3, that oxidize 5-methylcytosine (5mC) sequentially to 5-hydroxymethylcytosine (5hmC), 5-formylcytosine (5fC) and 5-carboxylcytosine (5caC) (He et al., 2011; Ito et al., 2010, 2011; Tahiliani et al., 2009). The roles of Tet enzymes were well documented in *in vivo* and *in vitro* study. Tet1 plays important roles in pluripotency and differentiation of embryonic stem cells (ESCs) (Ito et al., 2010; Koh et al., 2011; Yang et al., 2016), development, female meiosis (Yamaguchi et al., 2012) and tumorigenesis (Wu and Zhang, 2017). Both Tet1 and Tet2 are involved in lineage differentiation and pluripotency of ESCs (Khoueiry et al., 2017; Koh et al., 2011; Pastor et al., 2013; Williams et al., 2011; Wu et al., 2018), while Tet3 is indispensable for embryo epigenetic reprogramming (Gu et al., 2011; Wossidlo et al., 2011). Tet2 is also widely expressed in a variety of somatic organs and cell types, especially in hematopoietic cells (Moran-Crusio et al., 2011). *Tet1/2/3* triple knockout mice are embryonic lethal with severe gastrulation defects (Dai et al., 2016; Li et al., 2016).

[1]Department of Cell Biology and Genetics, College of Life Sciences, Nankai University, Tianjin 300071, China

[2]State Key Laboratory of Medicinal Chemical Biology, Nankai University, Tianjin 300071, China

[3]State Key Laboratory of Molecular Biology, Shanghai Institute of Biochemistry and Cell Biology, Chinese Academy of Sciences, Shanghai 200031, China

[4]These authors contributed equally

[5]Lead Contact

*Correspondence: glxu@sibcb.ac.cn (G.-L.X.), liulin@nankai.edu.cn (L.L.)

https://doi.org/10.1016/j.isci.2020.100908

However, *Tet1* or *Tet2* knockout mice are viable (Ko et al., 2011), suggesting that they are redundant for embryo development. Loss of both *Tet1* and *Tet2* enzymes is compatible with development but promotes hypermethylation and compromises imprinting, and most double mutant mice die perinatally, suggesting that these enzymes have overlapping roles in development (Dawlaty et al., 2013). Tet1 regulates meiotic gene expression and loss of *Tet1* causes female meiosis defect in fetal ovaries (Yamaguchi et al., 2012). Nevertheless, *Tet1* knockout mice are fertile albeit displaying reduced body mass and smaller litter size suggesting a subtle role for Tet1 in animal physiology (Dawlaty et al., 2011). Like *Tet1*, *Tet2* is dispensable for embryonic development and adult mutants also are fertile.

Although genome-wide DNA methylation studies have shown that in most tissue types in humans, methylation associated with promoters increases with age, and genome-wide DNA methylation decreases, 5hmC can be acquired or lost in different regions (Torano et al., 2016). The decline in age-dependent overall 5mC levels is consistent with previously known age-related genome-wide hypomethylation (Fuke et al., 2004; Heyn et al., 2012; Wilson et al., 1987). The level of 5hmC in human blood cells decreases with age, and some of them were associated with TET2 mutations. The reduction of 5hmC is much greater than the reduction of 5mC (Buscarlet et al., 2016). Multiple tissue DNA methylation epigenetic clocks are age-related. However, it remains elusive whether TET enzymes play a regulatory role in aging in the adult.

Moreover, hormonal differences in mice affect "biological age", as shown by accelerated epigenetic aging in ovariectomized mice (Stubbs et al., 2017). During spermatogenesis, 5hmC level is changed dynamically and correlated with gene expression, and RNAseq data shows that *Tet1* gene is expressed in spermatogonia (Gan et al., 2013; Hammoud et al., 2014; Nettersheim et al., 2013). The role of Dnmt1, 5mC, and 5hmC in the mammalian germline is to facilitate DNA demethylation and meiosis at the appropriate time (Hargan-Calvopina et al., 2016). Moreover, *Tet1* expression levels during human spermatogenesis also decease with age and are associated with reduced fertility (Ni et al., 2016). However, loss of *Tet1* in male mice minimally affects testis morphology and function or fertility, but leads to dysregulation of imprinted genes and a mild developmental delay shown as smaller body size (Dawlaty et al., 2011). Thus far, the function of *Tet* in male spermatogenesis and during aging remains to be explored. Given the importance of stem cell aging in the degeneration and dysfunction of aging tissues and the reversible nature of epigenetic regulation, a comprehensive understanding of the epigenetics of stem cell aging is central to the basic biology of aging (Chen and Kerr, 2019). Using *Tet*-deficient mice, we show that *Tet1* deficiency accelerates spermatogonial stem cell aging and leads to premature reproductive aging in males. Male mice deficient in *Tet1* exhibit progressive loss of germ cells, meiosis defect, increased apoptosis and subfertility with age. Furthermore, the mechanisms of Tet1 in regulating stem cell aging were investigated.

RESULTS

Tet1 Deficiency Reduces Male Fertility with Age

Heterozygous *Tet1* or *Tet2* mice (Zhang et al., 2013) were intercrossed to obtain *Tet1* knockout ($Tet1^{-/-}$) or *Tet2* knockout ($Tet2^{-/-}$) and control wild-type (WT) mice. Genotyping by PCR (Figure S1A) indicated that $Tet1^{-/-}$ mice were derived at the unexpected Mendelian frequency, with approximately a half of the number as expected, and this was consistent with a previous report (Yamaguchi et al., 2012). Quantitative real-time PCR showed that *Tet1* mRNA was expressed but at low level relative to GAPDH in WT testis and *Tet1* mRNA could not be detected in $Tet1^{-/-}$ testis (Figure S1B). We further determined the genotypes by immunofluorescence of Tet1 (green) and Oct4 (Red) in the developed embryos (Figure S1C). Consistent with loss of *Tet1*, dot-blot analyses showed a reduction of 5-hydroxymethylcytosine (5hmC) levels in $Tet1^{-/-}$ testis (Figure S1D). Co-immunofluorescence staining of 5hmC and 5mC followed by standard exposure time demonstrated that 5hmC strongly stained cells consistent with Sertoli cells and peritubular myoid cells, smooth muscle cells-like, by their locations (Figure S1E). Absolute quantification of 5hmC of mouse spermatogenic cells isolated from neonatal mice demonstrated that the Sertoli cells indeed had higher 5hmC content than male germ cells while mESC had a 5hmC content similar to spermatogonia cells (Gan et al., 2013). In contrast, 5mC moderately stained spermatogonia and spermatocytes. Moreover, 5mC fluorescence intensity was increased in $Tet1^{-/-}$ young (3 month-old) and old (11month-old) mouse tubules, compared with young (3 month-old) WT tubules. By overexposure of 5hmC staining, 5hmC expression could be revealed in the spermatogonia and spermatocytes of young WT tubules, and was reduced in $Tet1^{-/-}$ young and old mouse tubules (Figure S1F). Reduction of 5hmC if any in Sertoli cells and myoid cells after *Tet1* deficiency is not obvious likely due to high expression of 5hmC and partly to the

overexposure-caused exaggeration. Collectively, these data indicate that *Tet1* is effectively abolished and the low 5hmC expression level in spermatogonia and spermatocytes is further reduced in *Tet1*$^{-/-}$ testis.

Immunofluorescence of 5mC or 5hmC showed that 5mC staining can be found in different cell types including spermatogonia, spermatocytes and spermatid and that Tet1 deficiency generally increased 5mC fluorescence. Yet, 5hmC immunostaining pattern was intriguing. The question was whether the low fluorescence signal of 5hmC in spermatogonia and spermatocytes in WT tubules, and overall reduced 5hmC staining in *Tet1*$^{-/-}$ tubules and old mouse tubules represents real 5hmC expression level. Immunohistochemistry of cytosine modifications in human testes sections showed that levels of 5hmC are decreasing as spermatogenesis proceeds, while 5mC levels remain constant, indicate that during spermatogenesis active DNA demethylation becomes downregulated leading to a conservation of the methylation marks in mature sperm (Nettersheim et al., 2013). To estimate the 5mC and 5hmC levels in spermatogonia cells, we performed co-immunostaining using promyelocytic leukemia zinc-finger (PLZF) as a marker of undifferentiated spermatogonia (Buaas et al., 2004; Costoya et al., 2004; Hobbs et al., 2012), a less abundant spermatogonia population containing spermatogonial stem cells (SSCs) (Fayomi and Orwig, 2018). Spermatogonia cells are enriched in neonatal mouse testis (Gan et al., 2013), but very few cells in tubules were stained positive for PLZF in adult testis, as shown in a recent study (Grive et al., 2019). We observed that 5hmC levels in spermatogonia decrease in 11 month-old mice, compared with 3 month-old mice (Figures S2A and S2B). Furthermore, 5mC levels are increased but 5hmC levels reduced in *Tet1*$^{-/-}$ spermatogonia of young and old mice, compared with those of age-matched WT mice (Figures S2A–S2D), consistent with the well-established role of Tet1 in DNA demethylation, now shown also in spermatogonia.

To investigate the effects of *Tet* deficiency on male reproductive aging, we set up mating with young WT females of *Tet1*$^{-/-}$, or *Tet2*$^{-/-}$ males compared with WT males at three age groups (3 month-, 8 month- and 11 month-old) and counted the produced viable progeny after observing successful mating by plug next morning. The average litter size of WT males was slightly reduced with age, and did not reach significant difference by the age of 11 months, consistent with robust reproductive performance of hybrid male mouse strains. Compared to WT mice, loss of *Tet1* in males reduced ($p < 0.05$) number of pups at young age (3 month) and at the age of 8 months. But by 11 month-old, *Tet1*$^{-/-}$ males produced markedly ($p < 0.001$) reduced number of pups compared to age-matched WT males (Figure 1A). While WT mice produced litter size of an average of 8 pups at the 11 month-old, *Tet1*$^{-/-}$ males had only about 3 pups. This shows that the effect of loss of *Tet1* on male reproduction is age-related. Testis weight is an important reproductive trait in males. Consistent with age-related decline in fertility, the testis of *Tet1*$^{-/-}$ males was getting smaller with age, in contrast to WT mouse testes that became slightly larger with age. *Tet1*$^{-/-}$ males had significantly lighter testis than did age-matched WT males (Figures 1B and 1C).

Tet2 Deficiency Has Only Minor Effect on Male Fertility with Age

To know whether *Tet2* also may regulate male germ cell function with age, we examined fertility of *Tet2*$^{-/-}$ males with age, compared with age-matched WT controls. Genotyping by PCR indicated *Tet2* deficiency in *Tet2*$^{-/-}$ mice and normal *Tet2* in WT (Figure S3A). By qPCR, *Tet2* mRNA was expressed at low level relative to GAPDH in WT testis and *Tet2* mRNA level was minimal in *Tet2*$^{-/-}$ testis (Figure S3B). Moreover, immunofluorescence of Tet2 and synaptonemal complex protein 3 (Sycp3) in testis sections showed that Tet2 was not detectable in the testis of *Tet2*$^{-/-}$ mice and that both *Tet2*$^{-/-}$ and WT mice exhibited similar staining of Sycp3 positive cells, indicative appropriate homologous pairing. Tet2 was expressed mainly in primary spermatocytes, secondary spermatocytes and round spermatids (Figure S3C). 5mC and 5hmC immunofluorescence intensity was slightly changed following *Tet2* deficiency (Figure S3E).

Loss of *Tet2* in males slightly reduced number of pups at young age (3 month-old) but did not reach significant difference, compared to WT mice (Figure 1A). By the age of 8 month or 11 month-old, *Tet2*$^{-/-}$ males produced number of pups comparable to that of age-matched WT males (Figure 1A). The weight of *Tet2*$^{-/-}$ testis did not differ from that of WT mouse testes at the age of 3 or 8 month-old, but became lighter compared to WT when the mice reached the age of 11 months (Figure S3D). H&E staining of cross-sections of testis revealed that normal spermatogenesis were observed in most of seminiferous tubules of *Tet2*$^{-/-}$ males (Figure S3F). Only few seminiferous tubules of *Tet2*$^{-/-}$ mice showed reduced germ cells. These results suggest that the effect of loss of *Tet2* on male reproduction and aging is insignificant.

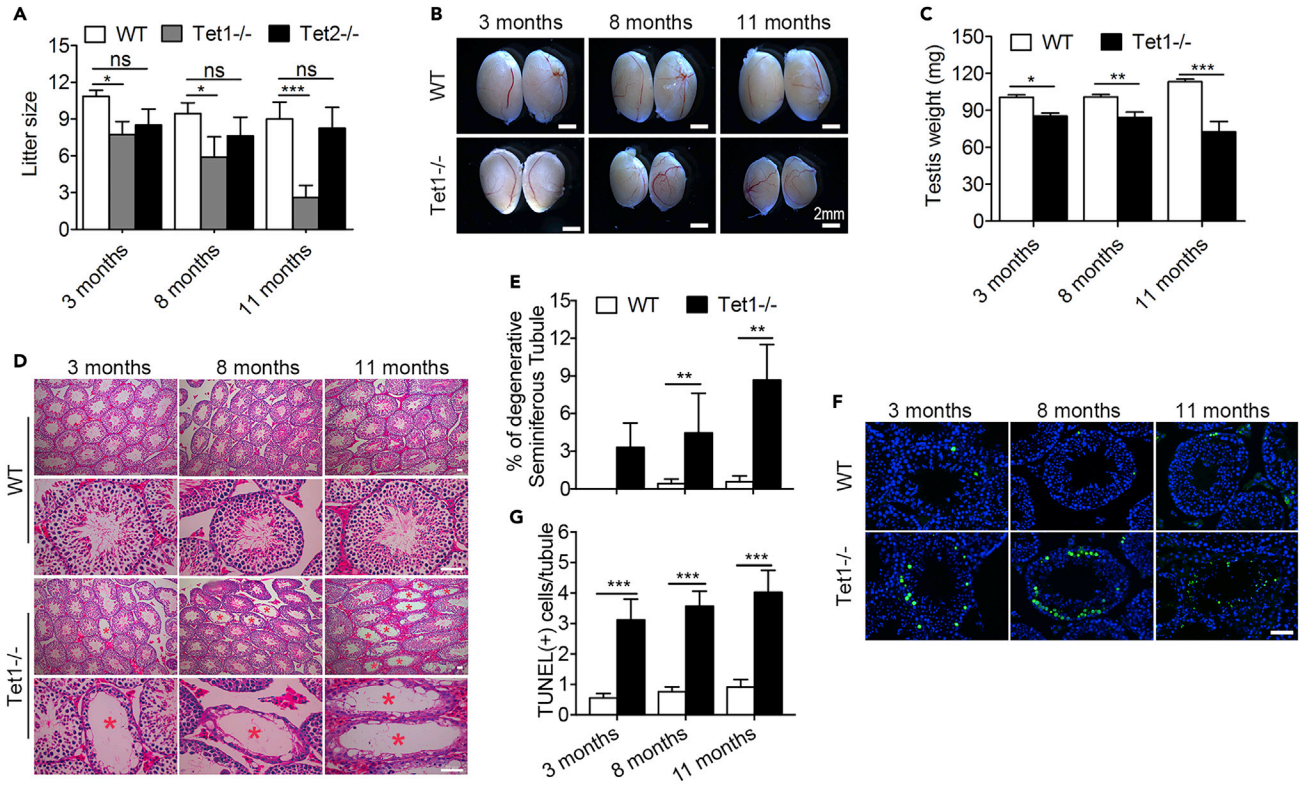

Figure 1. *Tet1*-Deficient Males Show Progressive Reduction in Fertility with Age and Spermatogenesis Defects

(A) Reduction in the fertility in *Tet1*$^{-/-}$ male mice with age, but not in *Tet2*$^{-/-}$ males, compared with WT males. Experiments were repeated at least three times for each age group males. n ≥ 8 males that had successful mating by the presence of plug with young female mice (2-3 months) were counted for number of pups produced (litter size) and evaluation of fertility. Data are represented as mean ± SEM.

(B) Representative images showing the testis collected from WT and *Tet1*$^{-/-}$ mice.

(C) Average testis weight. n = 8 mice for each group. Data are represented as mean ± SD.

(D and E) H&E-staining of the cross sections of seminiferous tubules from 3-, 8- and 11-month-old WT and *Tet1*$^{-/-}$ mice (D). Red asterisks represent tubules with loss of germ cells. (E) The ratios of degenerated tubules to the total number of tubules are presented. Four mice for each group were used. Scale bar, 50 μm. Data are represented as mean ± SD.

(F and G) Representative images (F) and quantification (G) of TUNEL positive cells in WT and *Tet1*$^{-/-}$ testes at 3, 8 and 11 months of age. Scale bar, 50 μm. Three mice for each group were used. Approximately 70 tubules each group were randomly counted. Green, apoptotic cells by TUNEL assay; Blue, nuclei stained with DAPI. Data are represented as mean ± SEM.*$p < 0.05$, **$p < 0.01$, ***$p < 0.001$, ns, not significant ($p > 0.05$). Student's t-test for A, C, E and G. See also Figures S1–S4.

Tet1 Deficiency Causes Progressive Loss of Germ Cells with Age

To understand the causes of subfertility with age in *Tet1*$^{-/-}$ mice, we examined histology of testes by H&E staining of cross-sections and immunofluorescence microscopy. Seminiferous tubules with disrupted spermatogenesis were observed in testes of *Tet1*$^{-/-}$ males. Some seminiferous tubules of *Tet1*$^{-/-}$ mice lacked a number of germ cell types such as round spermatid, and others were even depleted of germ cells, but only contained Sertoli cells. The percentage of degenerated tubules increased with age in *Tet1*$^{-/-}$ mice (Figures 1D and 1E). At the age of 3 month-old, about 3.3% tubules with disrupted spermatogenesis were observed, with increasing to 4.5% and 8.6% at the age of 8 months and 11 months (n = 4, four testes from four different mice examined at each age, respectively). Degenerated seminiferous tubules were not observed in testes of control WT males at 3 months and very few at the age of 8 months and 11months. Concurrent with degenerated seminiferous tubules in *Tet1*$^{-/-}$ males, a significant increase in germ cell apoptosis was observed. The TUNEL assay showed that the number of germ cell underwent apoptosis per tubule increased slightly in WT males with age, but increased significantly ($p < 0.001$) in *Tet1*$^{-/-}$ males when compared to age-matched WT males (Figures 1F and 1G). This result suggests that increased apoptosis is probably a contributing factor for progressive germ cell loss in *Tet1*$^{-/-}$ males, and this phenotype is age-related.

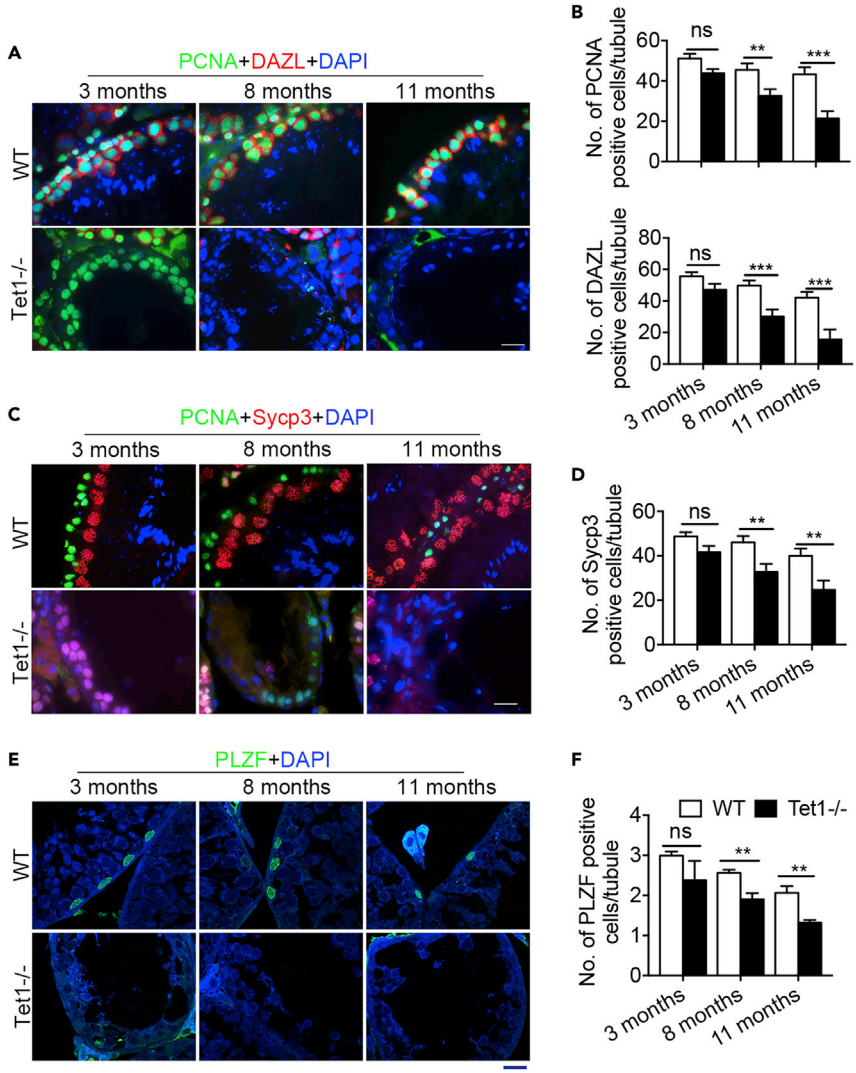

Figure 2. *Tet1* Deficiency Leads to Loss of Male Germ Cells with Age

(A) Sections of WT and *Tet1*$^{-/-}$ testis were co-stained with antibodies specific for PCNA (green) and DAZL (red).

(B) Number of PCNA and DAZL positive cells per seminiferous tubule. n = 10 tubules, three repeats.

(C) Sections of WT and *Tet1*$^{-/-}$ testis were co-stained with antibodies specific for PCNA (green) and Sycp3 (red).

(D) Number of Sycp3 positive cells per seminiferous tubule. n = 10 tubules, three repeats.

(E) Immunofluorescence of PLZF (green) in the sections of WT and *Tet1*$^{-/-}$ testis. DAPI (in blue) stains nucleus.

(F) Number of PLZF positive cells per seminiferous tubule. n = 20 tubules, three repeats. Data are represented as mean ± SEM. **p < 0.01, ***p < 0.001, ns, not significant (p > 0.05). Student's t-test for B, D, and F. Scale bar, 20 μm.

See also Figures S2 and S4.

To further confirm the loss of germ cells in the degenerative seminiferous tubules, we examined the expression of proliferating cell nuclear antigen (PCNA), a marker for proliferative cells (Wrobel et al., 1996), and used Dazl to reveal germ cells or Sycp3 to detect prophase I spermatocytes (Yuan et al., 2000). Both the numbers of PCNA and Dazl positive cells were significantly reduced in *Tet1*$^{-/-}$ mouse testis and further declined with age, compared to WT testis (Figures 2A and 2B). Normal seminiferous tubules of testes in *Tet1*$^{-/-}$ mice still had PCNA and Sycp3 positive cells, but the degenerative tubules showed very few PCNA and Sycp3 positive cells and other types of germ cell such as round sperm (Figures 2A and 2B). Furthermore, the number of PCNA positive spermatogonia and Sycp3 positive prophase I spermatocytes per seminiferous tubule both were significantly ($p < 0.001$) decreased in *Tet1*$^{-/-}$ mice compared to age-matched WT mice (Figures 2C and 2D). Hence, these results indicate that lack of *Tet1* leads to a progressive germ cell loss and spermatogenesis defect with age.

Adult stem cells play essential roles in maintenance of tissue homeostasis and regeneration. In mouse testis, SSCs are able to self-renew and differentiate, maintaining the continuous spermatogenesis to produce spermatozoa (Fayomi and Orwig, 2018; Kubota and Brinster, 2018). Because some complete degeneration of the seminiferous epithelium with a Sertoli cell-only phenotype was observed in *Tet1*$^{-/-}$ testis and *Tet1* was expressed in spermatogonia (containing SSCs) (Gan et al., 2013), this inspired us to hypothesize that loss of *Tet1* might impact self-renewal of SSCs, causing a progressive loss of germ cells with age. To substantiate this hypothesis, we carefully examined and compared PLZF positive cells between *Tet1*$^{-/-}$ and WT seminiferous tubules. Interestingly, the number of PLZF positive cells per seminiferous tubule also was decreased in WT mice with age, and significantly decreased in *Tet1*$^{-/-}$ mice compared to age-matched WT mice (Figures 2E and 2F). Previous findings also showed reduced number and proliferation of SSCs with age (Schmidt et al., 2011). Overall, these results indicate that loss of *Tet1* results in exhaustion of undifferentiated spermatogonia and degenerative tubules, suggesting that *Tet1* plays an important role in maintaining SSCs.

Tet1 Deficiency Leads to Meiosis Defect with Age

As shown above, *Tet1*$^{-/-}$ testis has morphologically normal tubules, so we asked whether they undergo meiosis correctly in these tubules. We tested whether loss of *Tet1* leads to meiosis defect with age. Co-immunostaining of spermatocytes spreads with the meiotic synapsis proteins Sycp3 and Sycp1 revealed that progression of meiotic prophase I was impaired in *Tet1*$^{-/-}$ males. At the age of 3 months, the percentage of leptotene and pachytene did not differ between *Tet1*$^{-/-}$ and WT males, but the percentage of zygotene in *Tet1*$^{-/-}$ males was increased, and the percentage of diplotene was decreased, compared with WT mice. At the age of 11 month-old, the percentage of leptotene and zygotene both were higher, and the percentage of diplotene was lower in *Tet1*$^{-/-}$ mice than in WT mice (Figures 3A and 3B).

Although changes in the percentage of four stages of prophase I spermatocytes indicated that the progression of meiosis prophase I was impaired in *Tet1*$^{-/-}$ males, no defect was observed in synapsis formation at pachytene stage. We asked whether *Tet1*$^{-/-}$ deficiency influences DNA repair and recombination. At the meiosis prophase I, meiotic recombination is essential for accurate segregation of homologous chromosomes (Hunter, 2015). The initiating event of meiotic recombination is a programmed DNA double-strand breaks (DSBs) introduced to the genome by Spo11 (Keeney et al., 1997). The DSBs which can be detected by the presence of γH2AX, must be subsequently repaired to form crossovers or noncrossovers (Gray and Cohen, 2016). As expected, many DSBs were present from leptotene to zygotene stages both in WT and *Tet1*$^{-/-}$ spermatocytes, and staining of γH2AX nearly disappeared at autosome except for XY body in pachytene and diplotene stage spermatocytes. However, staining of γH2AX still remained at autosome in some pachytene stage spermatocytes (termed as γH2AX positive cells), and the percentage of γH2AX positive pachytene cells was increased in *Tet1*$^{-/-}$ males at the age of 11 months compared to WT males (Figures 3C and 3D). These data suggest that *Tet1* deficiency caused DSB repair defect. The increased apoptotic cell death might be partially caused by meiosis defects.

In line with a DSBs repair defect, Rad51, the DSBs repair associated recombinase (Baier et al., 2014; Bannister and Schimenti, 2004), exhibited more foci in pachytene spermatocytes of *Tet1*$^{-/-}$ than in age-matched WT males (Figures 3E and 3G). The presence of γH2AX and delayed removal of RAD51 in the chromosomes indicate that homologous recombination and repair were still occurring, but impaired in *Tet1*$^{-/-}$ spermatocytes. MLH1 is an important marker for meiotic recombination and represents crossover (Baker et al., 1996; Guillon et al., 2005; Hassold et al., 2009). Co-immunostaining of spermatocytes surface spreads with Sycp3 and MLH1 showed that MLH1 foci decreased dramatically in pachytene spermatocytes of 11 month-old *Tet1*$^{-/-}$ males, but showed no difference at the age of 3 months (Figures 3F and 3H). Taken together, *Tet1* deficiency results in meiotic recombination defect with age.

Tet1 Deficiency Shortens Telomeres

Telomeres were shortened in mouse embryonic stem cells (ESCs) and in epiblast differentiation depleted of *Tet1* (Khoueiry et al., 2017; Yang et al., 2016), but it is unclear whether *Tet1* loss leads to telomere shortening in male germ cell. We preformed telomere quantitative fluorescence *in situ* hybridization (QFISH) and immunofluorescence of PLZF and Sycp3 on testis section and spermatocytes. Telomeres slightly shortened with age, and shortened further in *Tet1*$^{-/-}$ SSCs and pachytene spermatocytes, compared with those of WT mice (Figures S4A and 4B), which was further corroborated by Southern blot measurement of telomere TRF (Figure S4C). Although telomere length did not show dramatic reduction in the definite

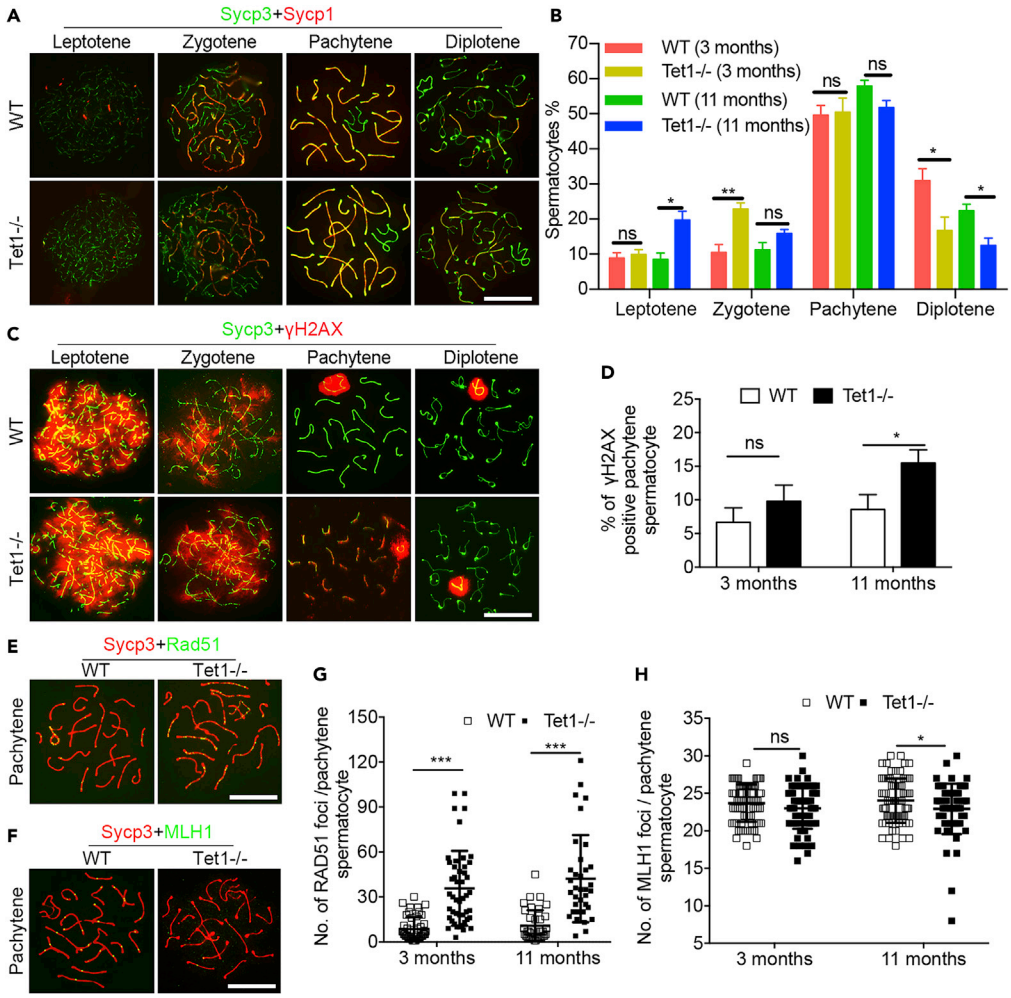

Figure 3. *Tet1* Deficiency Leads to Meiosis Defect with Age

(A) Co-immunofluorescence of Sycp3 (green) and Sycp1 (red) in spermatocytes. Scale bar, 20 μm.

(B) Frequencies of meiotic stages in WT and *Tet1*$^{-/-}$ testis suspensions. Approximately 200 meiocytes from 3-6 mice were counted for each stage.

(C) Co-immunofluorescence of Sycp3 (green) and γH2AX (red) in spermatocytes. Scale bar, 20 μm.

(D) Percentage of cells retaining γH2AX outside of the sex chromosomes in pachytene and diplotene spermatocytes. Approximately 50 pachytene meiocytes from 3 mice were counted.

(E and F) Co-immunofluorescence of Sycp3 (red) and Rad51(green) (E) or MLH1 (green, F) in spermatocytes. Scale bar, 20 μm.

(G) Quantification of the Rad51 foci per pachytene spermatocyte.

(H) Quantification of the MLH1 foci per pachytene spermatocyte. Approximately 30 pachytene meiocytes from three mice were counted. Data are represented as mean ± SEM. *$p < 0.05$, **$p < 0.01$, ***$p < 0.001$, ns, not significant ($p > 0.05$). Student's t-test for B, D, G, and H.

See also Figure S4.

spermatogonia and pachytene spermatocytes in *Tet1*$^{-/-}$ mice, these were survived cells, when used for preparation for telomere QFISH analysis, so they expectedly had better telomere maintenance. Others with shorter or dysfunctional telomeres might have undergone apoptosis that could not be detected due to the limitation of the assay.

Transcriptome Feature of Spermatogonia Cells with Age and Associated with *Tet1* Deficiency

During spermatogenesis, *Tet1* and *Tet2* are expressed at highest levels in type A & B spermatogonia, at reduced levels in primary spermatocytes and at minimal levels in spermatid, but *Tet3* is expressed at much higher levels than do *Tet1* and *Tet2* in all these cells (Gan et al., 2013). These data on spermatogonia

and spermatocytes were based on the materials obtained from neonatal mice. We attempted to localize Tet1 and Tet2 protein expression by immunofluorescence in these different cell types in the adult and aging males, and found that Tet2 protein is mainly expressed in primary and secondary spermatocytes and spermatid (Figure S2C). Unfortunately we could not reveal Tet1 localization by immunofluorescence staining, although we tested at least four Tet1 antibodies obtained commercially or custom-made. Next we explored the mechanism of *Tet1* in regulating male fertility by further assessing spermatogonia cells. We purified spermatogonia from testis by FACS and profiled their transcriptome by RNA-sequencing to investigate the molecular changes and mechanism after loss of *Tet1*. Based on cell sorting by Hoechst-blue and Hoechst red, P3 cell populations contained mostly spermatogonia cells, which took about 0.1-0.3% of whole cell populations (Figures S5A–S5D). Primary spermatocytes in P4 took about 1-5% of cell populations. P3 and P4 populations also were confirmed by co-immunofluorescence of Dnmt3b and absence of Sycp3, and Dnmt3b-negative and Sycp3-positive spermatocytes (Figure S5E). By immunofluorescence of PLZF, P3 cell populations after cell sorting contained few spermatocytes which were PLZF positive and had relatively large decondensed nuclei (Figure S5F). The purity of spermatogonia varied from 90%–98% each time.

We performed global principal component analysis (PCA) using transcripts per kilobase of exon model per million mapped reads (TPM) of all four groups: 3 month-old WT and *Tet1*$^{-/-}$, and 11 month-old WT and *Tet1*$^{-/-}$ mice. Transcriptome of spermatogonia from four groups could be mostly separated by clustering of PC1 and PC2 (Figure 4A), in which 11 month-old WT and 3 month-old *Tet1*$^{-/-}$ clustered close together, in consistency with correlation analysis, and the correlation coefficient of the two groups was up to 0.99 (Figure 4B). This is also consistent with Pearson's correlation coefficient diagram (Figure S5G). Specific genes were highly expressed in each group and also on chromosome Y shown by pheatmap in young male mice at the age of 3 month-old and were down-regulated in 3 month- *Tet1*$^{-/-}$ and 11 month- WT and 11 month-old *Tet1*$^{-/-}$ mice (Figures 4C and S5H). These data indicated that genes expressed in spermatogonia cells mostly were down-regulated after *Tet1* deficiency, and suggested that *Tet1* loss could accelerate the reproductive aging by impairing spermatogonia cells.

We enriched the genes by KOBAS (Xie et al., 2011), which were downregulated in 3 month-old *Tet1*$^{-/-}$ and 11 month-old WT and *Tet1*$^{-/-}$ mice. The GO results showed that these genes were enriched in spermatogenesis (29 genes), male gamete generation (29 genes), germ cell development (12 genes) and gamete generation (30 genes) (Figure 4D), based on the database of GO (http://geneontology.org/). Genes enriched in spermatogenesis and germ cell development were shown by pheatmap, and both exhibited higher expression in 3 months WT group, compared with other three groups (Figure 4E). We also looked at the enrichment of genes highly expressed in the 11 months old *Tet1*$^{-/-}$ mice. These genes were enriched in the categories of transcription factor activity, sequence-specific DNA binding, nucleic acid binding transcription factor activity, membrane, immune system process and cell differentiation (Figures 4F and 4G). These data show that *Tet1* deficiency accelerates spermatogonia cell aging.

Differential Gene Expression in Spermatogonia in Young and Old Males

To explore transcriptome changes during natural aging of spermatogonia cells, we further selected and performed RNA-seq analysis of 3 month and 11 month-old male mice. By analysis of differentially expressed genes (up: log2Foldchange >1, p value<0.05; down: log2Foldchange < -1, p value<0.05), 3,449 genes were highly expressed in 3 month-old WT males, in contrast to only 125 highly expressed genes in 11 month-old WT males, indicating that the expression of most genes decreased with age (Figure S6A and S6B), including *Dppa3*, *Cyp26b1*, *Kitl* and *Aurkc*. Dppa3/Stella as germline pluripotency marker is expressed at highest levels in one cluster of spermatogonia stem cells (Law et al., 2019), and activates spermatogenesis-associated genes (Dong et al., 2017). Elimination of Cyp26b1 activity within both germ and Sertoli cells resulted in severe male subfertility, with a loss of advanced germ cells from the seminiferous epithelium, indicating that Cyp26 activity within either Sertoli or germ cells is essential for the normal progression of spermatogenesis (Hogarth et al., 2015; Saba et al., 2014). Reduction of *Cyp26b1* could alter meiosis differentiation.

Genes downregulated in 11-month-old WT males were enriched in PI3K-Akt signaling pathway, retinol metabolism, cAMP signaling and AMPK signaling pathway (Figures S6C and S6D). PI3K-Akt signaling pathway regulates the proliferation and differentiation of SSCs (Zhou et al., 2015). AMPK and Wnt signaling pathway were all highly expressed in 3 month-old WT mice. GO enrichment results showed that genes

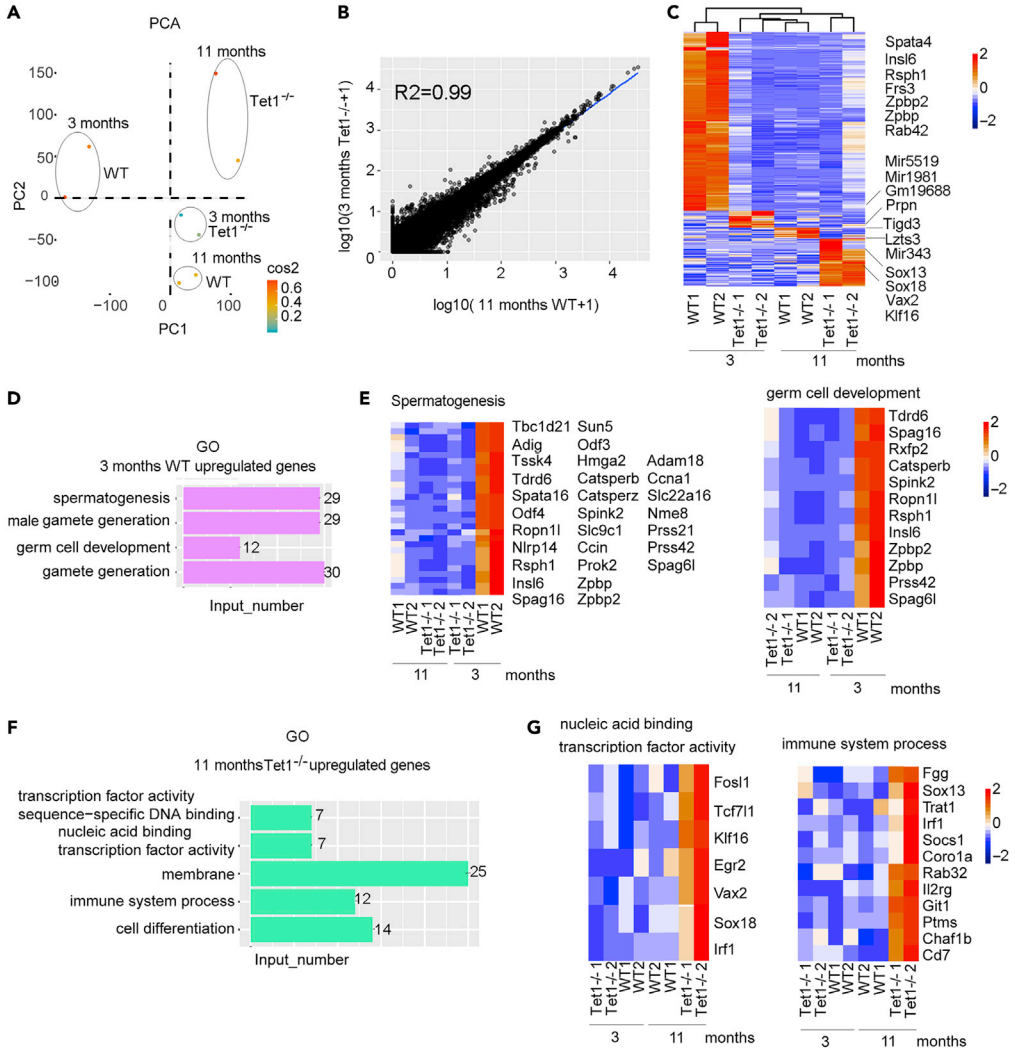

Figure 4. Transcriptome Feature of Spermatogonia Cells following *Tet1* Deficiency or Aging

(A) PCA analysis of TPM showing differential gene expression pattern among 3 month-old WT and *Tet1*$^{-/-}$, and 11 month-old WT and *Tet1*$^{-/-}$ spermatogonia and few spermatocytes.

(B) Correlation analysis. X axis represented the log10(TPM+1) of 11 month-old WT group, and Y axis represented the 1og10(TPM+1) of 3 month-old *Tet1*$^{-/-}$ spermatogonia cells. Their correlation coefficient was 0.99.

(C) Differential gene expression profile shown by pheatmap.

(D) GO enrichment analysis of specific genes with high expression levels in 3 month-old WT mice.

(E) Pheatmap showing the genes enriched in spermatogenesis and germ cell development.

(F) GO enrichment analysis of specific genes with high expression levels in 11 month-old *Tet1*$^{-/-}$ males.

(G) Pheatmap illustrating the genes enriched in nucleic acid binding transcription factor activity and immune system process.

See also Figures S5 and S6.

downregulated in 11 months WT group were focused on reproductive structure development, meiotic cell cycle, chromatin organization, cellular response to DNA damage stimulus, and actin cytoskeleton (Dunleavy et al., 2019) (Figure S6E), which play important roles in spermatogonia differentiation. Genes enriched in chromatin organization and meiotic cell cycle are shown by pheatmap (Figure S6F). Notably, *Spo11, Ccna1, Piwil1, Syce1l, Aurka,* and *Haspin* etc. were consistently downregulated in spermatogonia cells in old mice. SSC subtypes contain six clusters, and cluster 1 is highly enriched for categories of sexual reproduction, meiosis, and gametogenesis and includes *Piwil1, Sohlh2, Mael, Stra8, Rad51, Sycp,* and *Syce* (Hammoud et al., 2015). Meiotic genes are DNA methylated in PGCs but fully DNA-hypomethylated in adult SSCs (and "poised" by low/moderate H3K4me3) (Hammoud et al., 2014). Single-cell RNA-seq

identified four spermatogonial subtypes expressing many different markers for undifferentiated (e.g., *Gfra1, Lin28, Id4, Pax7, Etv5, Zbtb16*, and *Tert*) and differentiating spermatogonia (e.g., *Kit, Stra8, Sycp1, Sycp3, Dmrts*, and *Sohlhs*) (Green et al., 2018). Together, natural aging negatively affects transcriptome of spermatogenesis in mice.

Roles of *Tet1* on Spermatogonia

Next question was how *Tet1* regulates the aging of spermatogonia cells. We analyzed RNA-seq data from spermatogonia of 3 month-old *Tet1*$^{-/-}$ males and compared with the age-matched WT males. Scatter diagram showed that more genes were highly expressed in the 3-month-old WT males than in *Tet1*$^{-/-}$ males, indicating that the expression of most genes decreased after *Tet1* deficiency, including *Prdm8*, *Spo11*, *Aurka*, *Piwil1*, *Haspin* (Figure 5A). Other genes including *Casp3*, which plays important roles in apoptosis, and *Cacng6* were highly expressed in *Tet1*$^{-/-}$ males. There were 2,918 genes downregulated and only 43 upregulated in *Tet1*$^{-/-}$ males, compared to WT males, shown by pheatmap (Figure 5B). Spermatogonial cells express germ cell marker genes and meiotic marker genes (Sharma et al., 2019). Interestingly, genes important for meiosis progression, *Spo11*, *Piwil1*, *Ccna1*, *Hspa2*, and *Dnmt3l* were downregulated in *Tet1*$^{-/-}$ deficient germ cells, like those of natural aging (Figure 5C). As the third *Piwi* family member, *Piwil1*, also known as *Miwi*, is specifically highly expressed in adult testis and essential for spermatogenesis (Deng and Lin, 2002; Yue et al., 2014). Piwil1/Miwi is required for the continued maintenance of repeat-derived piRNAs long after transposon silencing is established in germline stem cells and is essential for male fertility (Reuter et al., 2011). Genes downregulated in *Tet1*$^{-/-}$ males were enriched in PI3K-Akt signaling pathway, cAMP signaling, AMPK signaling, MAPK signaling and retinol metabolism (Figures 5D and 5E), like those of aging mice shown above.

GO enrichment results showed that genes downregulated in 3 month-old *Tet1*$^{-/-}$ males were focused on spermatogenesis, sexual reproduction, microtubule cytoskeleton, meiosis I cell cycle phase, and germ cell development (Figures 5F and 5G), indicating that *Tet1* deficiency leads to abnormal spermatogenesis. Similar effects of age and *Tet1* deficiency on specific pathways together with PCA data suggest that *Tet1* deficiency mimics aging-associated dysfunction in spermatogenesis.

Methylation Aging Clock of Germ Cells

Methylation aging clock has been proposed and validated in somatic cell aging (Horvath, 2013; Horvath and Raj, 2018). Mouse aging clock appeared to differ from human aging clock by comparison analysis (Figure 6A). Previous studies have shown that male germ cells in adult mice have highly different methylation state (Cui et al., 2016; Gan et al., 2013), and different patterns of epigenetic dysregulation in DNA methylation occur in tissue-specific over time (Thompson et al., 2010), but how methylation plays a role in spermatogonia and germ cells aging remains to be determined. DNA methylation of transcription start site (TSS) usually suppresses gene transcription (review (Xiao et al., 2019)). We overlapped the genes with high expression in 3 month-old mouse WT spermatogonia but low expression presumably associated with methylation in 11-month old WT males and 3 month-old *Tet1*$^{-/-}$ and 11 month-old *Tet1*$^{-/-}$ spermatogonia, with mouse (Thompson et al., 2018) and human aging clock genes (including 253 genes in mice and 345 genes in humans) (Lu et al., 2019) (Figure 6A). Interestingly, only two genes *Aldh3b1* and *Fam50b* that are highly expressed in the 3 month-old mice but lower expressed in 11 month-old WT males and 3 month-*Tet1*$^{-/-}$ and 11 month-old *Tet1*$^{-/-}$ males (Figure 6B), overlapped with aging clock genes in humans, and only *Ppp1r36* overlapped with the mouse aging clock genes. *Tet1* deficiency or age can lead to a significant decline in the expression of both genes.

To understand whether these two genes are regulated by methylation, we used the Integrative Genomics Viewer (IGV) to see if 5hmC regulates the promoter of *Aldh3b1*. H3K4me3 is used to show the promoter region of the gene (i.e. the gray region in Figure 6C), from which it can be seen that 5hmC is bound to the *Aldh3b1* promoter region regardless of type A or B-type spermatogonia cells, and the signal binding to the coding exon of *Aldh3b1* was stronger. This suggests that the expression of *Aldh3b1* could be regulated by 5hmC. It has been shown that 5hmC is enriched in gene bodies and proximal promoters but depleted in intergenic regions and TSS in spermatogonia and spermatocytes and the study further provided evidence for a positive regulatory role of 5hmC in gene activation during spermatogenesis (Gan et al., 2013). Additionally, we compared the abundance of Tet1, 5hmC and 5mC on *Aldh3b1*. Tet1 is bound to the promoter of *Aldh3b1* in WT spermatogonia, but the binding reduced in *Tet1*$^{-/-}$ spermatogonia (Figure 6C). Binding of 5hmC on *Aldh3b1* in ES cells is similar to that of spermatogonia cells, on both the promoter and exon of *Aldh3b1*. Signal of 5hmC on the intergenic and coding of

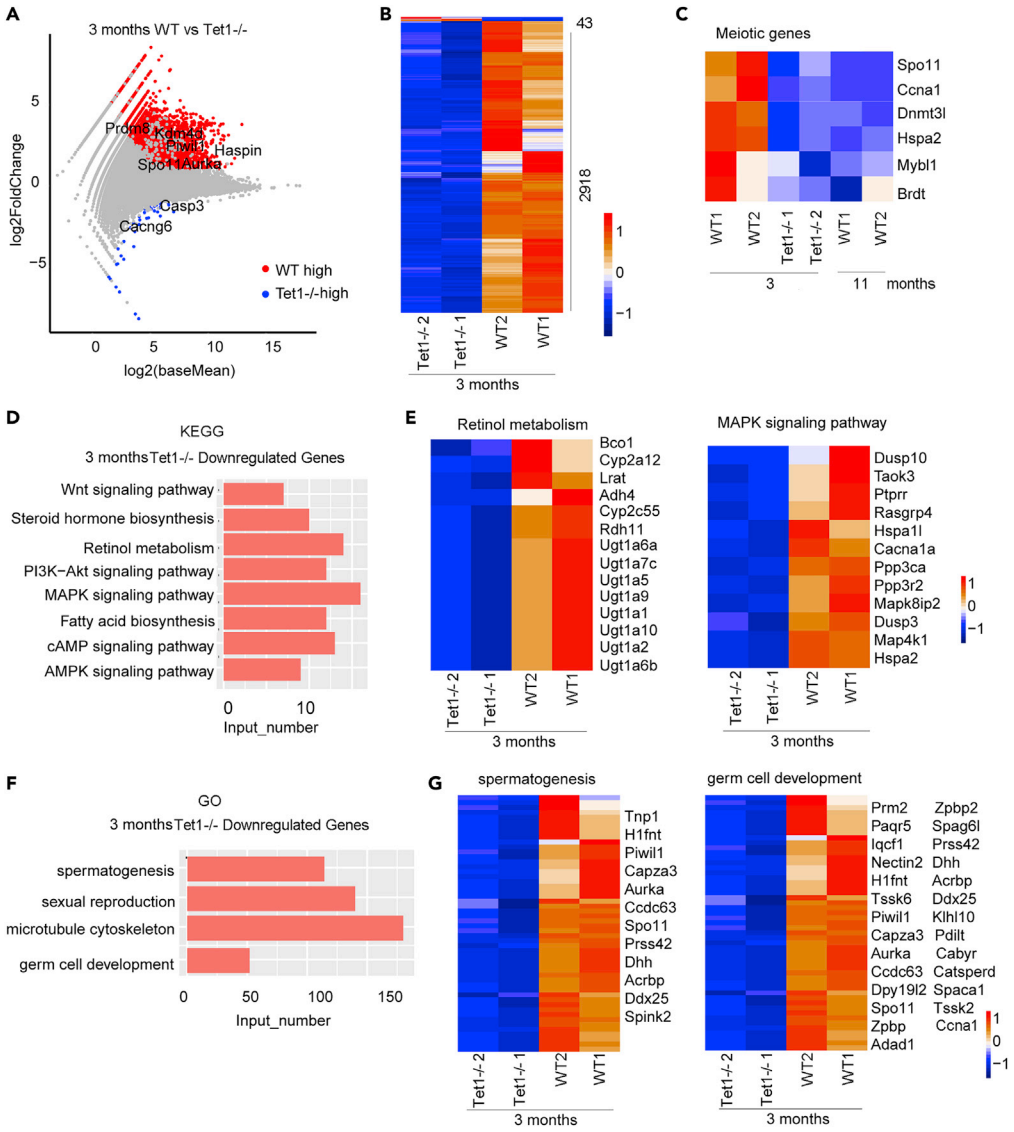

Figure 5. *Tet1* Deficiency Alters Transcriptome of Germ Cells

(A) Scatterplot showing differential gene expression between 3 months WT and *Tet1*$^{-/-}$ spermatogonia and spermatocytes. Red represents genes with higher expression in 3 months WT, and blue represents genes with higher expression in *Tet1*$^{-/-}$, gray represented no significance between 3 month and *Tet1*$^{-/-}$ spermatogonia and spermatocytes.

(B) Differential gene expression shown by pheatmap. Differential genes were selected by the standard of log2Foldchange>1 or log2Foldchange < -1, and p value < 0.05.

(C) Pheatmap showing meiotic related genes including *Spo11*, *Ccna1* and *Dnmt3l* that are downregulated.

(D) KEGG results enriched by the 2,918 genes downregulated in 3 months *Tet1*$^{-/-}$ spermatogonia and spermatocytes by KOBAS websites.

(E) Pheatmap showing the genes enriched in retinal metabolism and MAPK signaling pathway.

(F) GO results enriched by the 2,918 genes downregulated in 3 months *Tet1*$^{-/-}$ spermatogonia and spermatocytes.

(G) Pheatmap showing the genes enriched in spermatogenesis and germ cell development (http://zfin.org/action/ontology/term-detail/GO:0007281).

See also Figure S6.

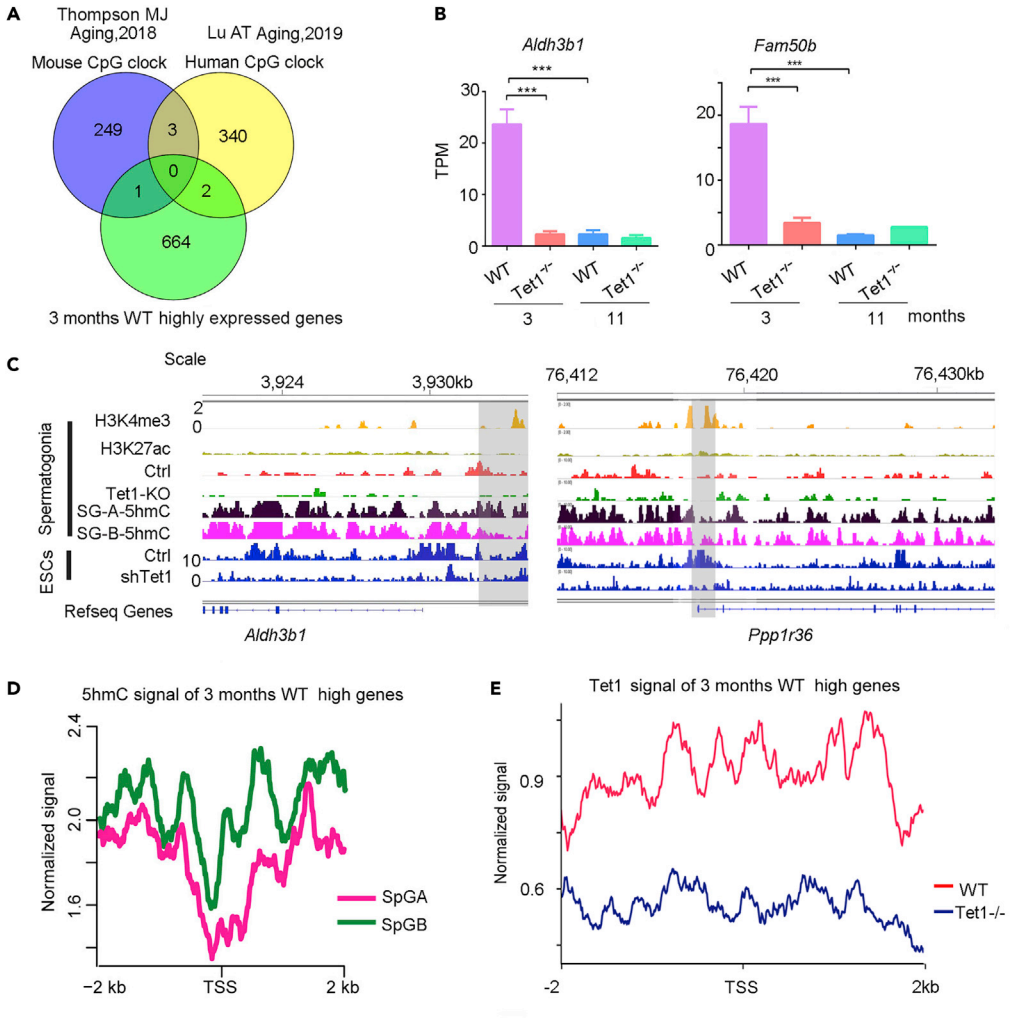

Figure 6. Transcriptome of Spermatogonia Cells and Methylation Aging Clock

(A) Venn diagram in comparison of highly expressed genes in 3 month-old WT mice but downregulated in other three groups shown in Figure 4C, with methylation aging clock of mouse (Thompson et al., 2018) and human genes (Lu et al., 2019).

(B) Bar plot showing *Aldh3b1* and *Fam50b* expressed at significantly higher levels in 3 months WT group. Data are represented as mean ± SEM. (n = 3). ***p < 0.001, Student's t-test.

(C) Integrative Genomics Viewer (IGV) demonstrating binding site of *Aldh3b1*and *Ppp1r36*. H3K4me3 was used to show the promoter location of *Aldh3b1*. Tet1 biding to the Control and *Tet1* knockout spermatogonia cells (our data) is compared with 5hmC enrichment in both type A and type B spermatogonia cells. Tet1 abundance in ESCs and *Tet1* knocked down ESCs served another control. H3K4me3 and H3K27me3 data were obtained from (Hammoud et al., 2014), SG-A-5hmC and SG-B-5hmC from (Gan et al., 2013), and Tet1-Ctrl and shTet1 from (Williams et al., 2011).

(D) Average signal level of 5hmC binding to 667 genes in 3 months WT near TSS region of the spermatogonia cells. Pink represents Type A spermatogonia cells and green represents Type B spermatogonia cells.

(E) Average signal level of Tet1 binding to 667 genes in 3 months WT near TSS region. The signal was decreased in *Tet1* knockout spermatogonia cells.

See also Figure S7.

Ppp1r36 in spermatogonia cells also is strong. These data suggest that *Aldh3b1* and *Ppp1r36* could be regulated by Tet1 and its mediated-5hmC.

To determine whether reproductive cell aging have its own unique clock or pattern, we analyzed 5hmC signals at 667 genes highly expressed in the 3-month WT group in spermatogonia cells but with lower expression in other three groups. 5hmC strongly bound to intergenic and intragenic region of the genes but

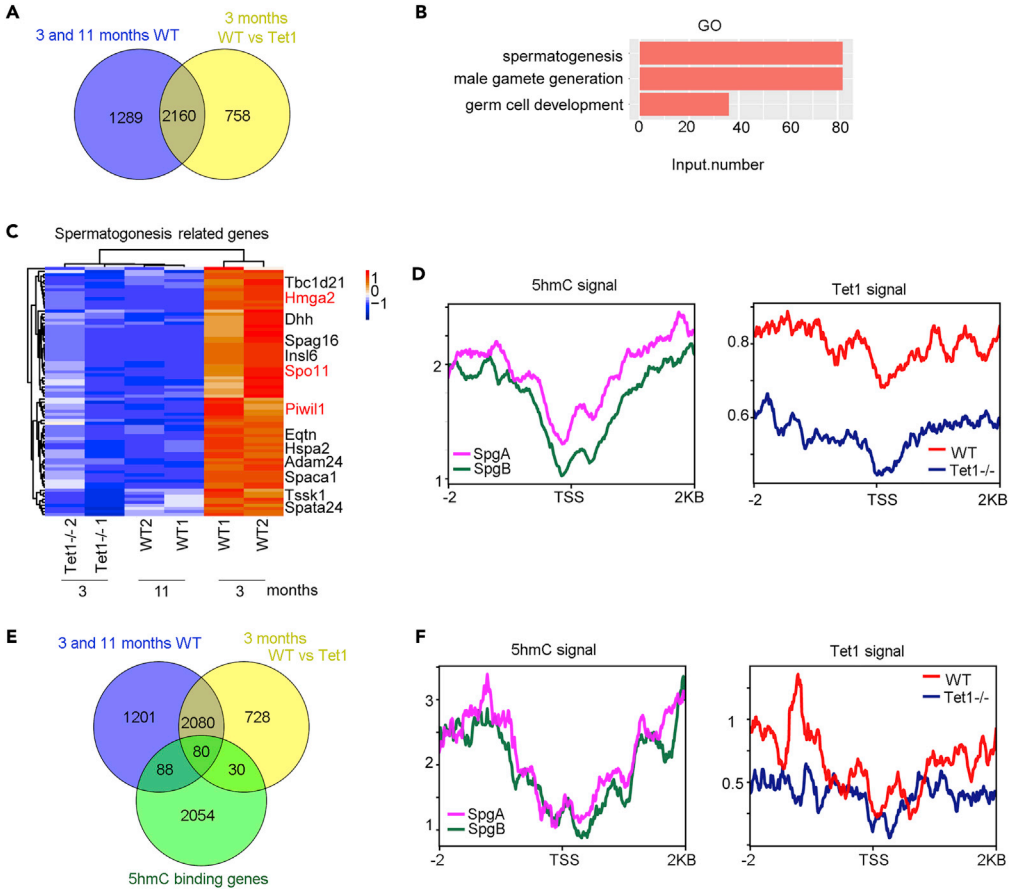

Figure 7. ChIP-seq Analysis of the Genes Downregulated with Age and *Tet1* Deficiency

(A) Venn diagram showing the genes downregulated in 3 month-old WT vs 11 month-old WT, or 3 month-old WT vs *Tet1*$^{-/-}$ spermatogonia cells.

(B) GO enrichments of the downregulated genes in spermatogenesis, gamete generation and germ cell development.

(C) Pheatmap illustrating the genes related to spermatogenesis that are highly expressed in 3 month-old WT mice.

(D) Average signal of 5hmC or Tet1 by ChIP-seq on the genes downregulated in both *Tet1*$^{-/-}$ and 11 month-old spermatogonia cells.

(E) Venn diagram showing the genes downregulated in 3 months WT vs 11 months WT, or 3 months WT vs *Tet1*$^{-/-}$ spermatogonia cells, and 80 of them are shared by 5hmC binding.

(F) Average signal of 5hmC or Tet1 on the 80 shared genes in spermatogonia cells.

See also Figure S7.

reduced at the promoter region (near TSS) of spermatogonia cells (Figure 6D). However, Tet1 could bind to both TSS as well as intergenic and intragenic region of these genes, and the binding to these regions was noticeably reduced in *Tet1*$^{-/-}$ spermatogonia (Figure 6E). These data suggest that both Tet1 and 5hmC are involved in transcriptional regulation of these genes in spermatogonia cells. It remains to be validated whether these genes can mark germ cell aging clock. Nevertheless, from our initial analysis, aging clock of somatic cells may differ from that of germ cells.

Mechanism of Transcriptional Regulation by *Tet1* and Age on Spermatogonia Cells

Based on the data analysis shown above, there were more down-regulated genes than up-regulated genes in 11 month-old WT and 3 month-old *Tet1*$^{-/-}$ males compared with 3 month-old WT males. We tested the hypothesis that *Tet1* deficiency may lead to premature senility of mouse spermatogonia cells. We draw a Venn diagram of these down-regulated genes, showing that 2,160 genes were both downregulated in 3 month *Tet1*$^{-/-}$ and 11 month-old WT spermatogonia cells (Figure 7A). GO results showed that these 2,160 genes were enriched in spermatogenesis, gamete generation and germ cell development (Figure 7B). Genes associated with spermatogenesis were downregulated in 3 month-old *Tet1*$^{-/-}$ and

11 month-old WT spermatogonia cells (Figure 7C). Normalized 5hmC signal of type A and type B spermatogonia was decreased in TSS region. Tet1 signal also decreased in TSS region and the signal of Tet1 on the genes in WT spermatogonia cells were noticeably reduced in *Tet1*$^{-/-}$ spermatogonia cells (Figure 7D), implying similarly regulatory mechanisms of these genes by 5hmC and Tet1. We also analyzed the genes downregulated in 3 month-old *Tet1*$^{-/-}$ and 11 month-old WT spermatogonia cells and the genes with 5hmC binding, which revealed 80 genes overlapped among them (Figure 7E). Again, 5hmC or Tet1 signal on the 80 genes shared was decreased in TSS region. Signal of Tet1 on these genes in WT spermatogonia cells also were reduced in *Tet1*$^{-/-}$ spermatogonia cells but to less extent (Figure 7F). These data suggested that reduction of 5hmC and Tet1 can contribute to the declined expression of the genes associated with spermatogenesis with age or *Tet1* deficiency.

Further comparison of 5hmC binding genes in ESCs (Williams et al., 2011), type A and type B spermatogonia (Gan et al., 2013), revealed that there were 1,920 genes common in ESCs and spermatogonia cells, and 2,375 genes in the spermatogonia A and B cell types (Figure S7A). These genes are involved in various signaling transduction pathways and biological functions (Figures S7B–S7D). Again, 99 genes downregulated in 3 month-old *Tet1*$^{-/-}$ and 11 month-old WT mice were co-occupied by 5hmC in both ESCs and spermatogonia cells (Figures S7E and S7F). While 5hmC signal in the TSS region of these genes was decreased, the signal of Tet1 in the TSS region of the genes was elevated in spermatogonia cells, but reduced in *Tet1*$^{-/-}$ spermatogonia cells (Figure S7G). These data support the notion that Tet1 has a role in transcriptional regulation of the bound genes. *Tet1* deficiency can result in declined expression of its bound genes.

DISCUSSION

We provide a direct evidence to demonstrate the link of Tet enzyme to aging. In this study, we present an important role of Tet enzymes in reproductive aging using knockout mouse model, which has advantages in study of aging in general. We have shown that Tet enzyme and its intermediate product 5hmC regulate germline and stem cell aging. Although *Tet1* or *Tet2* deficiency leads to reduced 5hmC and increased 5mC to similar levels, compared with wild-type mice, they result in differential impact on reproductive aging and perhaps aging in general. It is likely that transcriptional regulation by Tet1 in combination with methylation/demethylation together regulate reproductive aging.

Increasing evidence shows reduced levels of 5hmC and Tet enzymes with age and these suggest their potential participation in aging. Aging is associated with decreased *TET1* and *TET2* expression (Jessop and Toledo-Rodriguez, 2018). *Tet1* expression levels also decease with age and are associated with reduced fertility (Ni et al., 2016), as shown here in mice. Similarly, a decrease in *Tet2* expression and 5hmC levels was detected in the aged hippocampus associated with adult neurogenesis (Gontier et al., 2018). An age-related decline of TET1, TET3 and TDG gene expression along with a decrease of 5hmC and an accumulation of 5caC, and the observed impairment of 5hmC-mediated DNA demethylation pathway in blood cells may lead to aberrant transcriptional programs in the elderly (Valentini et al., 2016). Also, it has been demonstrated that 5hmC content decreased with age in the peripheral blood T cells, and that the mRNA expression levels of TET1 and TET3 decreased with age, while those of TET2 were not influenced by age (Truong et al., 2015). In contrast, evidence also is reported that global 5hmC content was increased during aging in the absence of 5mC decrease, suggesting that 5hmC could act as an epigenetic marker and not only as an intermediary in DNA demethylation (Chen et al., 2012). Similar to cerebrum, the human cerebellum shows an age-dependent increase in 5hmC content, although at lower absolute levels (Wagner et al., 2015), consistent with others suggesting that increased 5hmC may play a role in age-related neurodegeneration (Song et al., 2011; Szulwach et al., 2011). However, age-related changes in DNA hydroxymethylation could be more complicated, and cell type specific and gene specific (Kochmanski et al., 2018). These age-correlated observations also could not determine whether levels of 5hmC or Tet enzymes contribute to aging, or are the result of aging.

We intended to address these questions by using *Tet* knockout mice as prove of principles. We sought firstly to investigate whether *Tet* deficiency can actually cause premature aging using *Tet* knockout mice as a model, and then to understand how *Tet* deficiency and/or 5hmC levels accelerates aging. To shorten the observation period, here we focused on reproductive aging in males.

Indeed, our data reveals that Tet1 plays a major role in regulating reproductive aging unlike Tet2. *Tet1* deficiency results in reduced expression of genes, like those of natural aging. The genes downregulated in aging males or in *Tet1*-deficient males are enriched in in spermatogonia cell cycle progression,

spermatogenesis, meiosis, germ cell differentiation and DNA repair etc. For instance, *Ccna1* expression is greatly reduced in *Tet1*-deficient males, like that of natural reproductive aging males, compared with young mice. Ccna1 (Cyclin A1) is expressed in mice exclusively in the germ cell lineage and is required for meiosis in the male mouse. *Ccna1*$^{-/-}$ males were sterile due to a block of spermatogenesis before the first meiotic division, whereas females were normal. Meiosis arrest in *Ccna1*$^{-/-}$ males was associated with increased germ cell apoptosis and desynapsis abnormalities (Liu et al., 1998). *Ccna1*$^{+/-}$ male mice also show reduced sperm production and fertility (van der Meer et al., 2004). Reduced expression of *Ccna1* following *Tet1* deficiency could negatively affect self-renewal of spermatogonia cells and delays meiotic cell cycle, consistent with the observation that PLZF-positive spermatogonia cells are greatly reduced in *Tet1*-deficient males and in natural aging. Also, *Spo11*, critical for meiosis homologous pairing and recombination initiation (Boateng et al., 2013; Keeney et al., 1997), is down-regulated in *Tet1*-deficient spermatogonia and spermatocytes, like that of natural reproductive aging males. We observed significantly delayed meiosis progression and homologous pairing and recombination in *Tet1*-deficient meiocytes. DNA methyltransferase 3-like (*Dnmt3L*) is expressed in SSCs and their precursors. Loss of *Dnmt3L* from early germ cells also caused meiotic failure in spermatocytes and infertility (Bourc'his and Bestor, 2004). In *Dnmt3L*$^{-/-}$ meiotic spermatocytes, homologous chromosomes fail to align and form synaptonemal complexes, spermatogenesis arrests, and spermatocytes are lost by apoptosis and sloughing (Webster et al., 2005).

Moreover, aldehyde dehydrogenase (ALDH) enzymes are critical in the detoxification of aldehydes. ALDH3B1 belongs to the ALDH3 family and protects cells from the damaging effects of oxidative stress (Marchitti et al., 2010). Ppp1r36, a regulatory subunit of protein phosphatase 1, is highly enriched in human (Fagerberg et al., 2014) and mouse testis, and enhances autophagy during spermatogenesis (Zhang et al., 2016). These genes showed significant reduction in the expression in both *Tet1* deficient mice and old mice. It is also interesting to note that both *Tet1* deficient mice and natural aging mice showed similarly declined signal pathways, including Wnt, Retinol metabolism, Ras/MAPK, PI3K-Akt, and AMPK. These are involved in aging, or spermatogonia stem cell proliferation (Griswold, 2016; Grive et al., 2019; Takase and Nusse, 2016). *Tet1*$^{-/-}$ spermatogonia cells had abnormal retinol metabolism, reducing meiosis entry (Bowles et al., 2006; Feng et al., 2014). MAPK signaling pathway plays a key role in maintaining self-renewal capacity of mouse male germline stem cells (Gao et al., 2018; Hasegawa et al., 2013). Actually, mutations dysregulating RAS-MAPK signaling are often found in aged human testes (Maher et al., 2018). It is likely that reduced expression of these important genes and defective signaling pathways together contribute to accelerated reproductive aging resulting from *Tet1* deficiency, similar to natural aging.

Telomere shortening also leads to aging or accelerated aging (Armanios et al., 2009; Armanios and Blackburn, 2012; Blackburn et al., 2015; Blasco, 2005). High telomerase is a hallmark of undifferentiated spermatogonia and is required for maintenance of male germline stem cells (Pech et al., 2015). Telomerase activity is expressed at high levels in the type A spermatogonial stem cells, is down-regulated during spermatogenesis, and is absent in the differentiated spermatozoa (Ravindranath et al., 1997). Tet enzyme also is involved in the regulation of telomere length in mouse ESCs and epiblasts (Khoueiry et al., 2017; Lu et al., 2014; Yang et al., 2016). In epiblast cells, Tet1 demethylates gene promoters via hydroxylation of 5mC and maintains telomere stability (Khoueiry et al., 2017). We show that telomeres are shortened in spermatogonia cells as well as in spermatocytes of *Tet1* deficient mice.

Our study highlights an interplay between the catalytic and non-catalytic activities of Tet1 that plays important role in regulating transcription of spermatogonia and spermatogenesis, contributing to both normal development and aging. Generally, DNA methylation in regions near the TSS is closely associated with the suppression of gene expression (Xiao et al., 2019). Tet1 and Tet2 function to regulate locus-specific methylation during PGC development. *Tet* depletion induces promoter and gene body hypermethylation that is consistent with 5hmC having a locus-specific role in DNA demethylation in PGCs (Hackett et al., 2013; Vincent et al., 2013). There is a possibility that reduced expression of genes related to germ cells and spermatogenesis might result from hypermethylation when *Tet1* is deficient. There has been very little information on how the age-related changes in DNA methylation affect the transcriptome or function of a tissue or cell. Methylation changes, in association with reduced RNA expression levels, in germ cells with age or following *Tet1* deficiency, may not be the same as those in blood which strongly predicts lifespan and healthspan (Lu et al., 2019). Tissues have heterogeneous cell populations, and it is well established that different cell types have different epigenetic profiles. The effect of aging on DNA methylation could be

cell-type specific. TET1 stimulates transcription of germline reprogramming-responsive genes via a DNA demethylation-independent mechanism, thus enabling progression toward gametogenesis (Hill et al., 2018). Despite reduced gene expression, methylation levels of spermatogenesis-related promoters remain relatively stable, and no substantial difference in the global DNA methylation patterns was observed between 18 week and 17 month samples (Kobayashi et al., 2016). Our data shows that 5hmC also does not enrich at the TSS of those genes downregulated with age or due to *Tet1* deficiency in male germline cells. Whether spermatogonia cells may have their unique methylome aging marks requires further investigation.

Limitations of the Study

Tet1 knockout decreases 5hmC levels in spermatogonia cells and downregulates a clear set of genes important for cell cycle progression, germ cell differentiation, meiosis and reproduction, such as *Ccna1* and *Spo11*. Furthermore, Tet1 and 5hmC both regulate signaling pathways important for stem cell development, retinol metabolism, MAPK, PI3K-Akt, and AMPK, etc. These gene expression changes were obtained by bioinformatics analysis of RNA-seq data and in partial combination with ChIP-seq data. Further experiments will be needed to look at whether the gene expression can actually lead to changes at the protein levels by proteomics analysis and by western blot.

METHODS

All methods can be found in the accompanying Transparent Methods supplemental file.

DATA AND CODE AVAILABILITY

Data and code related to this paper may be requested from the authors. Raw RNA-seq sequences are available online (https://www.ncbi.nlm.nih.gov/geo/query/acc.cgi?acc=GSE140014) and raw ChIP-seq sequences are available online (https://www.ncbi.nlm.nih.gov/geo/query/acc.cgi?acc=GSE140999). The accession number for the dataset reported in this paper is NCBI: [GSE140014 and GSE140999].

SUPPLEMENTAL INFORMATION

Supplemental Information can be found online at https://doi.org/10.1016/j.isci.2020.100908.

ACKNOWLEDGMENTS

This work was supported by the National Natural Science Foundation of China (31571546, 91749129).

AUTHOR CONTRIBUTIONS

G.H. designed and performed major experiments and prepared manuscript. L.L.L. analyzed the RNA-seq and CHIP-seq data. H.W. conducted major experiments. M.G. J.Y. and W.D. helped genotyping and other tests. P.G. assisted IF-FISH experiment. C.T. helped TRF and CHIP assay. T.Z provided reagents and materials. G.X. provided the Tet1 and Tet2 knockout mice, advised the study, and revised the manuscript. L.L. conceived the study, designed experiments and wrote the manuscript.

DECLARATION OF INTERESTS

The authors declare they have no competing interests.

Received: November 11, 2019
Revised: December 8, 2019
Accepted: February 7, 2020
Published: March 27, 2020

REFERENCES

Armanios, M., and Blackburn, E.H. (2012). The telomere syndromes. Nat. Rev. Genet. *13*, 693–704.

Armanios, M., Alder, J.K., Parry, E.M., Karim, B., Strong, M.A., and Greider, C.W. (2009). Short telomeres are sufficient to cause the degenerative defects associated with aging. Am. J. Hum. Genet. *85*, 823–832.

Baier, B., Hunt, P., Broman, K.W., and Hassold, T. (2014). Variation in genome-wide levels of meiotic recombination is established at the onset of prophase in mammalian males. PLoS Genet. *10*, e1004125.

Baker, S.M., Plug, A.W., Prolla, T.A., Bronner, C.E., Harris, A.C., Yao, X., Christie, D.M., Monell, C., Arnheim, N., Bradley, A., et al. (1996). Involvement of mouse Mlh1 in DNA mismatch repair and meiotic crossing over. Nat. Genet. *13*, 336–342.

Bannister, L.A., and Schimenti, J.C. (2004). Homologous recombinational repair proteins in

mouse meiosis. Cytogenet. Genome Res. *107*, 191–200.

Blackburn, E.H., Epel, E.S., and Lin, J. (2015). Human telomere biology: a contributory and interactive factor in aging, disease risks, and protection. Science *350*, 1193–1198.

Blasco, M.A. (2005). Telomeres and human disease: ageing, cancer and beyond. Nat. Rev. Genet. *6*, 611–622.

Boateng, K.A., Bellani, M.A., Gregoretti, I.V., Pratto, F., and Camerini-Otero, R.D. (2013). Homologous pairing preceding SPO11-mediated double-strand breaks in mice. Dev. Cell *24*, 196–205.

Bourc'his, D., and Bestor, T.H. (2004). Meiotic catastrophe and retrotransposon reactivation in male germ cells lacking Dnmt3L. Nature *431*, 96–99.

Bowles, J., Knight, D., Smith, C., Wilhelm, D., Richman, J., Mamiya, S., Yashiro, K., Chawengsaksophak, K., Wilson, M.J., Rossant, J., et al. (2006). Retinoid signaling determines germ cell fate in mice. Science *312*, 596–600.

Buaas, F.W., Kirsh, A.L., Sharma, M., McLean, D.J., Morris, J.L., Griswold, M.D., de Rooij, D.G., and Braun, R.E. (2004). Plzf is required in adult male germ cells for stem cell self-renewal. Nat. Genet. *36*, 647–652.

Buscarlet, M., Tessier, A., Provost, S., Mollica, L., and Busque, L. (2016). Human blood cell levels of 5-hydroxymethylcytosine (5hmC) decline with age, partly related to acquired mutations in TET2. Exp. Hematol. *44*, 1072–1084.

Chen, D., and Kerr, C. (2019). The epigenetics of stem cell aging comes of age. Trends Cell Biol. *29*, 563–568.

Chen, H., Dzitoyeva, S., and Manev, H. (2012). Effect of aging on 5-hydroxymethylcytosine in the mouse hippocampus. Restor. Neurol. Neurosci. *30*, 237–245.

Costoya, J.A., Hobbs, R.M., Barna, M., Cattoretti, G., Manova, K., Sukhwani, M., Orwig, K.E., Wolgemuth, D.J., and Pandolfi, P.P. (2004). Essential role of Plzf in maintenance of spermatogonial stem cells. Nat. Genet. *36*, 653–659.

Cui, X., Jing, X., Wu, X., Yan, M., Li, Q., Shen, Y., and Wang, Z. (2016). DNA methylation in spermatogenesis and male infertility. Exp. Ther. Med. *12*, 1973–1979.

Dai, H.Q., Wang, B.A., Yang, L., Chen, J.J., Zhu, G.C., Sun, M.L., Ge, H., Wang, R., Chapman, D.L., Tang, F., et al. (2016). TET-mediated DNA demethylation controls gastrulation by regulating Lefty-Nodal signalling. Nature *538*, 528–532.

Dawlaty, M.M., Ganz, K., Powell, B.E., Hu, Y.C., Markoulaki, S., Cheng, A.W., Gao, Q., Kim, J., Choi, S.W., Page, D.C., et al. (2011). Tet1 is dispensable for maintaining pluripotency and its loss is compatible with embryonic and postnatal development. Cell Stem Cell *9*, 166–175.

Dawlaty, M.M., Breiling, A., Le, T., Raddatz, G., Barrasa, M.I., Cheng, A.W., Gao, Q., Powell, B.E., Li, Z., Xu, M., et al. (2013). Combined deficiency of Tet1 and Tet2 causes epigenetic abnormalities but is compatible with postnatal development. Dev. Cell *24*, 310–323.

Deng, W., and Lin, H. (2002). miwi, a murine homolog of piwi, encodes a cytoplasmic protein essential for spermatogenesis. Dev. Cell *2*, 819–830.

Dong, G., Shang, Z., Liu, L., Liu, C., Ge, Y., Wang, Q., Wu, L., Chen, F., Li, B., Liu, X., et al. (2017). Retinoic acid combined with spermatogonial stem cell conditions facilitate the generation of mouse germ-like cells. Biosci. Rep. *37*, https://doi.org/10.1042/BSR20170637.

Dunleavy, J.E.M., O'Bryan, M., Stanton, P.G., and O'Donnell, L. (2019). The cytoskeleton in spermatogenesis. Reproduction *157*, R53–R72.

Fagerberg, L., Hallstrom, B.M., Oksvold, P., Kampf, C., Djureinovic, D., Odeberg, J., Habuka, M., Tahmasebpoor, S., Danielsson, A., Edlund, K., et al. (2014). Analysis of the human tissue-specific expression by genome-wide integration of transcriptomics and antibody-based proteomics. Mol. Cell. Proteomics *13*, 397–406.

Fayomi, A.P., and Orwig, K.E. (2018). Spermatogonial stem cells and spermatogenesis in mice, monkeys and men. Stem Cell Res. *29*, 207–214.

Feng, C.W., Bowles, J., and Koopman, P. (2014). Control of mammalian germ cell entry into meiosis. Mol. Cell. Endocrinol. *382*, 488–497.

Fuke, C., Shimabukuro, M., Petronis, A., Sugimoto, J., Oda, T., Miura, K., Miyazaki, T., Ogura, C., Okazaki, Y., and Jinno, Y. (2004). Age related changes in 5-methylcytosine content in human peripheral leukocytes and placentas: an HPLC-based study. Ann. Hum. Genet. *68*, 196–204.

Gan, H., Wen, L., Liao, S., Lin, X., Ma, T., Liu, J., Song, C.X., Wang, M., He, C., Han, C., et al. (2013). Dynamics of 5-hydroxymethylcytosine during mouse spermatogenesis. Nat. Commun. *4*, 1995.

Gao, T., Zhao, X., Liu, C., Shao, B., Zhang, X., Li, K., Cai, J., Wang, S., and Huang, X. (2018). Somatic angiotensin I-converting enzyme regulates self-renewal of mouse spermatogonial stem cells through the mitogen-activated protein kinase signaling pathway. Stem Cells Dev. *27*, 1021–1032.

Gontier, G., Iyer, M., Shea, J.M., Bieri, G., Wheatley, E.G., Ramalho-Santos, M., and Villeda, S.A. (2018). Tet2 rescues age-related regenerative decline and enhances cognitive function in the adult mouse brain. Cell Rep. *22*, 1974–1981.

Gray, S., and Cohen, P.E. (2016). Control of meiotic crossovers: from double-strand break formation to designation. Annu. Rev. Genet. *50*, 175–210.

Green, C.D., Ma, Q., Manske, G.L., Shami, A.N., Zheng, X., Marini, S., Moritz, L., Sultan, C., Gurczynski, S.J., Moore, B.B., et al. (2018). A comprehensive roadmap of murine spermatogenesis defined by single-cell RNA-seq. Dev. Cell *46*, 651–667.e10.

Greenberg, M.V.C., and Bourc'his, D. (2019). The diverse roles of DNA methylation in mammalian development and disease. Nat. Rev. Mol. Cell Biol. *20*, 590–607.

Griswold, M.D. (2016). Spermatogenesis: the commitment to meiosis. Physiol. Rev. *96*, 1–17.

Grive, K.J., Hu, Y., Shu, E., Grimson, A., Elemento, O., Grenier, J.K., and Cohen, P.E. (2019). Dynamic transcriptome profiles within spermatogonial and spermatocyte populations during postnatal testis maturation revealed by single-cell sequencing. PLoS Genet. *15*, e1007810.

Gu, T.P., Guo, F., Yang, H., Wu, H.P., Xu, G.F., Liu, W., Xie, Z.G., Shi, L., He, X., Jin, S.G., et al. (2011). The role of Tet3 DNA dioxygenase in epigenetic reprogramming by oocytes. Nature *477*, 606–610.

Guillon, H., Baudat, F., Grey, C., Liskay, R.M., and de Massy, B. (2005). Crossover and noncrossover pathways in mouse meiosis. Mol. Cell *20*, 563–573.

Hackett, J.A., Sengupta, R., Zylicz, J.J., Murakami, K., Lee, C., Down, T.A., and Surani, M.A. (2013). Germline DNA demethylation dynamics and imprint erasure through 5-hydroxymethylcytosine. Science *339*, 448–452.

Hammoud, S.S., Low, D.H., Yi, C., Carrell, D.T., Guccione, E., and Cairns, B.R. (2014). Chromatin and transcription transitions of mammalian adult germline stem cells and spermatogenesis. Cell Stem Cell *15*, 239–253.

Hammoud, S.S., Low, D.H., Yi, C., Lee, C.L., Oatley, J.M., Payne, C.J., Carrell, D.T., Guccione, E., and Cairns, B.R. (2015). Transcription and imprinting dynamics in developing postnatal male germline stem cells. Genes Dev. *29*, 2312–2324.

Hargan-Calvopina, J., Taylor, S., Cook, H., Hu, Z., Lee, S.A., Yen, M.R., Chiang, Y.S., Chen, P.Y., and Clark, A.T. (2016). Stage-specific demethylation in primordial germ cells safeguards against precocious differentiation. Dev. Cell *39*, 75–86.

Hasegawa, K., Namekawa, S.H., and Saga, Y. (2013). MEK/ERK signaling directly and indirectly contributes to the cyclical self-renewal of spermatogonial stem cells. Stem Cells *31*, 2517–2527.

Hassold, T., Hansen, T., Hunt, P., and VandeVoort, C. (2009). Cytological studies of recombination in rhesus males. Cytogenet. Genome Res. *124*, 132–138.

He, Y.F., Li, B.Z., Li, Z., Liu, P., Wang, Y., Tang, Q., Ding, J., Jia, Y., Chen, Z., Li, L., et al. (2011). Tet-mediated formation of 5-carboxylcytosine and its excision by TDG in mammalian DNA. Science *333*, 1303–1307.

Heyn, H., Li, N., Ferreira, H.J., Moran, S., Pisano, D.G., Gomez, A., Diez, J., Sanchez-Mut, J.V., Setien, F., Carmona, F.J., et al. (2012). Distinct DNA methylomes of newborns and centenarians. Proc. Natl. Acad. Sci. U S A *109*, 10522–10527.

Hill, P.W.S., Leitch, H.G., Requena, C.E., Sun, Z., Amouroux, R., Roman-Trufero, M., Borkowska, M., Terragni, J., Vaisvila, R., Linnett, S., et al. (2018). Epigenetic reprogramming enables the transition from primordial germ cell to gonocyte. Nature *555*, 392–396.

Hobbs, R.M., Fagoonee, S., Papa, A., Webster, K., Altruda, F., Nishinakamura, R., Chai, L., and Pandolfi, P.P. (2012). Functional antagonism between Sall4 and Plzf defines germline progenitors. Cell Stem Cell *10*, 284–298.

Hogarth, C.A., Evans, E., Onken, J., Kent, T., Mitchell, D., Petkovich, M., and Griswold, M.D. (2015). CYP26 enzymes are necessary within the postnatal seminiferous epithelium for normal murine spermatogenesis. Biol. Reprod. *93*, 19.

Horvath, S. (2013). DNA methylation age of human tissues and cell types. Genome Biol. *14*, R115.

Horvath, S., and Raj, K. (2018). DNA methylation-based biomarkers and the epigenetic clock theory of ageing. Nat. Rev. Genet. *19*, 371–384.

Hunter, N. (2015). Meiotic recombination: the essence of heredity. Cold Spring Harb. Perspect. Biol. *7*, a016618.

Ito, S., D'Alessio, A.C., Taranova, O.V., Hong, K., Sowers, L.C., and Zhang, Y. (2010). Role of Tet proteins in 5mC to 5hmC conversion, ES-cell self-renewal and inner cell mass specification. Nature *466*, 1129–1133.

Ito, S., Shen, L., Dai, Q., Wu, S.C., Collins, L.B., Swenberg, J.A., He, C., and Zhang, Y. (2011). Tet proteins can convert 5-methylcytosine to 5-formylcytosine and 5-carboxylcytosine. Science *333*, 1300–1303.

Jenkins, T.G., Aston, K.I., Pflueger, C., Cairns, B.R., and Carrell, D.T. (2014). Age-associated sperm DNA methylation alterations: possible implications in offspring disease susceptibility. PLoS Genet. *10*, e1004458.

Jenkins, T.G., Aston, K.I., Meyer, T., and Carrell, D.T. (2015). The sperm epigenome, male aging, and potential effects on the embryo. Adv. Exp. Med. Biol. *868*, 81–93.

Jessop, P., and Toledo-Rodriguez, M. (2018). Hippocampal TET1 and TET2 expression and DNA hydroxymethylation are affected by physical exercise in aged mice. Front. Cell Dev. Biol. *6*, 45.

Keeney, S., Giroux, C.N., and Kleckner, N. (1997). Meiosis-specific DNA double-strand breaks are catalyzed by Spo11, a member of a widely conserved protein family. Cell *88*, 375–384.

Khoueiry, R., Sohni, A., Thienpont, B., Luo, X., Velde, J.V., Bartoccetti, M., Boeckx, B., Zwijsen, A., Rao, A., Lambrechts, D., et al. (2017). Lineage-specific functions of TET1 in the postimplantation mouse embryo. Nat. Genet. *49*, 1061–1072.

Klutstein, M., Nejman, D., Greenfield, R., and Cedar, H. (2016). DNA methylation in cancer and aging. Cancer Res. *76*, 3446–3450.

Ko, M., Bandukwala, H.S., An, J., Lamperti, E.D., Thompson, E.C., Hastie, R., Tsangaratou, A., Rajewsky, K., Koralov, S.B., and Rao, A. (2011). Ten-Eleven-Translocation 2 (TET2) negatively regulates homeostasis and differentiation of hematopoietic stem cells in mice. Proc. Natl. Acad. Sci. U S A *108*, 14566–14571.

Kobayashi, N., Okae, H., Hiura, H., Chiba, H., Shirakata, Y., Hara, K., Tanemura, K., and Arima, T. (2016). Genome-scale assessment of age-related DNA methylation changes in mouse spermatozoa. PLoS One *11*, e0167127.

Kochmanski, J., Marchlewicz, E.H., Cavalcante, R.G., Sartor, M.A., and Dolinoy, D.C. (2018). Age-related epigenome-wide DNA methylation and hydroxymethylation in longitudinal mouse blood. Epigenetics *13*, 779–792.

Koh, K.P., Yabuuchi, A., Rao, S., Huang, Y., Cunniff, K., Nardone, J., Laiho, A., Tahiliani, M., Sommer, C.A., Mostoslavsky, G., et al. (2011). Tet1 and Tet2 regulate 5-hydroxymethylcytosine production and cell lineage specification in mouse embryonic stem cells. Cell Stem Cell *8*, 200–213.

Kubota, H., and Brinster, R.L. (2018). Spermatogonial stem cells. Biol. Reprod. *99*, 52–74.

Law, N.C., Oatley, M.J., and Oatley, J.M. (2019). Developmental kinetics and transcriptome dynamics of stem cell specification in the spermatogenic lineage. Nat. Commun. *10*, 2787.

Li, X., Yue, X., Pastor, W.A., Lin, L., Georges, R., Chavez, L., Evans, S.M., and Rao, A. (2016). Tet proteins influence the balance between neuroectodermal and mesodermal fate choice by inhibiting Wnt signaling. Proc. Natl. Acad. Sci. U S A *113*, E8267–E8276.

Liu, D., Matzuk, M.M., Sung, W.K., Guo, Q., Wang, P., and Wolgemuth, D.J. (1998). Cyclin A1 is required for meiosis in the male mouse. Nat. Genet. *20*, 377–380.

Lopez-Otin, C., Blasco, M.A., Partridge, L., Serrano, M., and Kroemer, G. (2013). The hallmarks of aging. Cell *153*, 1194–1217.

Lu, F., Liu, Y., Jiang, L., Yamaguchi, S., and Zhang, Y. (2014). Role of Tet proteins in enhancer activity and telomere elongation. Genes Dev. *28*, 2103–2119.

Lu, A.T., Quach, A., Wilson, J.G., Reiner, A.P., Aviv, A., Raj, K., Hou, L., Baccarelli, A.A., Li, Y., Stewart, J.D., et al. (2019). DNA methylation GrimAge strongly predicts lifespan and healthspan. Aging (Albany NY) *11*, 303–327.

Maher, G.J., Ralph, H.K., Ding, Z., Koelling, N., Mlcochova, H., Giannoulatou, E., Dhami, P., Paul, D.S., Stricker, S.H., Beck, S., et al. (2018). Selfish mutations dysregulating RAS-MAPK signaling are pervasive in aged human testes. Genome Res. *28*, 1779–1790.

Marchitti, S.A., Brocker, C., Orlicky, D.J., and Vasiliou, V. (2010). Molecular characterization, expression analysis, and role of ALDH3B1 in the cellular protection against oxidative stress. Free Radic. Biol. Med. *49*, 1432–1443.

Moran-Crusio, K., Reavie, L., Shih, A., Abdel-Wahab, O., Ndiaye-Lobry, D., Lobry, C., Figueroa, M.E., Vasanthakumar, A., Patel, J., Zhao, X., et al. (2011). Tet2 loss leads to increased hematopoietic stem cell self-renewal and myeloid transformation. Cancer Cell *20*, 11–24.

Nettersheim, D., Heukamp, L.C., Fronhoffs, F., Grewe, M.J., Haas, N., Waha, A., Honecker, F., Waha, A., Kristiansen, G., and Schorle, H. (2013). Analysis of TET expression/activity and 5mC oxidation during normal and malignant germ cell development. PLoS One *8*, e82881.

Ni, K., Dansranjavin, T., Rogenhofer, N., Oeztuerk, N., Deuker, J., Bergmann, M., Schuppe, H.C., Wagenlehner, F., Weidner, W., Steger, K., et al. (2016). TET enzymes are successively expressed during human spermatogenesis and their expression level is pivotal for male fertility. Hum. Reprod. *31*, 1411–1424.

Pastor, W.A., Aravind, L., and Rao, A. (2013). TETonic shift: biological roles of TET proteins in DNA demethylation and transcription. Nat. Rev. Mol. Cell Biol. *14*, 341–356.

Pech, M.F., Garbuzov, A., Hasegawa, K., Sukhwani, M., Zhang, R.J., Benayoun, B.A., Brockman, S.A., Lin, S., Brunet, A., Orwig, K.E., et al. (2015). High telomerase is a hallmark of undifferentiated spermatogonia and is required for maintenance of male germline stem cells. Genes Dev. *29*, 2420–2434.

Ravindranath, N., Dalal, R., Solomon, B., Djakiew, D., and Dym, M. (1997). Loss of telomerase activity during male germ cell differentiation. Endocrinology *138*, 4026–4029.

Reuter, M., Berninger, P., Chuma, S., Shah, H., Hosokawa, M., Funaya, C., Antony, C., Sachidanandam, R., and Pillai, R.S. (2011). Miwi catalysis is required for piRNA amplification-independent LINE1 transposon silencing. Nature *480*, 264–267.

Saba, R., Wu, Q., and Saga, Y. (2014). CYP26B1 promotes male germ cell differentiation by suppressing STRA8-dependent meiotic and STRA8-independent mitotic pathways. Dev. Biol. *389*, 173–181.

Schmidt, J.A., Abramowitz, L.K., Kubota, H., Wu, X., Niu, Z., Avarbock, M.R., Tobias, J.W., Bartolomei, M.S., and Brinster, R.L. (2011). In vivo and in vitro aging is detrimental to mouse spermatogonial stem cell function. Biol. Reprod. *84*, 698–706.

Sharma, S., Wistuba, J., Pock, T., Schlatt, S., and Neuhaus, N. (2019). Spermatogonial stem cells: updates from specification to clinical relevance. Hum. Reprod. Update *25*, 275–297.

Song, C.X., Szulwach, K.E., Fu, Y., Dai, Q., Yi, C., Li, X., Li, Y., Chen, C.H., Zhang, W., Jian, X., et al. (2011). Selective chemical labeling reveals the genome-wide distribution of 5-hydroxymethylcytosine. Nat. Biotechnol. *29*, 68–72.

Stubbs, T.M., Bonder, M.J., Stark, A.K., Krueger, F., Team, B.I.A.C., von Meyenn, F., Stegle, O., and Reik, W. (2017). Multi-tissue DNA methylation age predictor in mouse. Genome Biol. *18*, 68.

Szulwach, K.E., Li, X., Li, Y., Song, C.X., Wu, H., Dai, Q., Irier, H., Upadhyay, A.K., Gearing, M., Levey, A.I., et al. (2011). 5-hmC-mediated epigenetic dynamics during postnatal neurodevelopment and aging. Nat. Neurosci. *14*, 1607–1616.

Tahiliani, M., Koh, K.P., Shen, Y., Pastor, W.A., Bandukwala, H., Brudno, Y., Agarwal, S., Iyer, L.M., Liu, D.R., Aravind, L., et al. (2009). Conversion of 5-methylcytosine to 5-hydroxymethylcytosine in mammalian DNA by MLL partner TET1. Science *324*, 930–935.

Takase, H.M., and Nusse, R. (2016). Paracrine Wnt/beta-catenin signaling mediates proliferation of undifferentiated spermatogonia in the adult mouse testis. Proc. Natl. Acad. Sci. U S A *113*, E1489–E1497.

Tan, L., and Shi, Y.G. (2012). Tet family proteins and 5-hydroxymethylcytosine in development and disease. Development *139*, 1895–1902.

Thompson, R.F., Atzmon, G., Gheorghe, C., Liang, H.Q., Lowes, C., Greally, J.M., and Barzilai, N. (2010). Tissue-specific dysregulation of DNA methylation in aging. Aging Cell *9*, 506–518.

Thompson, M.J., Chwialkowska, K., Rubbi, L., Lusis, A.J., Davis, R.C., Srivastava, A., Korstanje, R., Churchill, G.A., Horvath, S., and Pellegrini, M. (2018). A multi-tissue full lifespan epigenetic clock for mice. Aging (Albany NY) *10*, 2832–2854.

Torano, E.G., Bayon, G.F., Del Real, A., Sierra, M.I., Garcia, M.G., Carella, A., Belmonte, T., Urdinguio, R.G., Cubillo, I., Garcia-Castro, J., et al. (2016). Age-associated hydroxymethylation in human bone-marrow mesenchymal stem cells. J. Transl. Med. *14*, 207.

Truong, T.P., Sakata-Yanagimoto, M., Yamada, M., Nagae, G., Enami, T., Nakamoto-Matsubara, R., Aburatani, H., and Chiba, S. (2015). Age-dependent decrease of DNA hydroxymethylation in human T cells. J. Clin. Exp. Hematop. *55*, 1–6.

Valentini, E., Zampieri, M., Malavolta, M., Bacalini, M.G., Calabrese, R., Guastafierro, T., Reale, A., Franceschi, C., Hervonen, A., Koller, B., et al. (2016). Analysis of the machinery and intermediates of the 5hmC-mediated DNA demethylation pathway in aging on samples from the MARK-AGE Study. Aging (Albany NY) *8*, 1896–1922.

van der Meer, T., Chan, W.Y., Palazon, L.S., Nieduszynski, C., Murphy, M., Sobczak-Thepot, J., Carrington, M., and Colledge, W.H. (2004). Cyclin A1 protein shows haplo-insufficiency for normal fertility in male mice. Reproduction *127*, 503–511.

Vincent, J.J., Huang, Y., Chen, P.Y., Feng, S., Calvopina, J.H., Nee, K., Lee, S.A., Le, T., Yoon, A.J., Faull, K., et al. (2013). Stage-specific roles for tet1 and tet2 in DNA demethylation in primordial germ cells. Cell Stem Cell *12*, 470–478.

Wagner, M., Steinbacher, J., Kraus, T.F., Michalakis, S., Hackner, B., Pfaffeneder, T., Perera, A., Muller, M., Giese, A., Kretzschmar, H.A., et al. (2015). Age-dependent levels of 5-methyl-, 5-hydroxymethyl-, and 5-formylcytosine in human and mouse brain tissues. Angew. Chem. Int. Ed. *54*, 12511–12514.

Webster, K.E., O'Bryan, M.K., Fletcher, S., Crewther, P.E., Aapola, U., Craig, J., Harrison, D.K., Aung, H., Phutikanit, N., Lyle, R., et al. (2005). Meiotic and epigenetic defects in Dnmt3L-knockout mouse spermatogenesis. Proc. Natl. Acad. Sci. U S A *102*, 4068–4073.

Williams, K., Christensen, J., Pedersen, M.T., Johansen, J.V., Cloos, P.A., Rappsilber, J., and Helin, K. (2011). TET1 and hydroxymethylcytosine in transcription and DNA methylation fidelity. Nature *473*, 343–348.

Wilson, V.L., Smith, R.A., Ma, S., and Cutler, R.G. (1987). Genomic 5-methyldeoxycytidine decreases with age. J. Biol. Chem. *262*, 9948–9951.

Wossidlo, M., Nakamura, T., Lepikhov, K., Marques, C.J., Zakhartchenko, V., Boiani, M., Arand, J., Nakano, T., Reik, W., and Walter, J. (2011). 5-Hydroxymethylcytosine in the mammalian zygote is linked with epigenetic reprogramming. Nat. Commun. *2*, 241.

Wrobel, K.H., Bickel, D., and Kujat, R. (1996). Immunohistochemical study of seminiferous epithelium in adult bovine testis using monoclonal antibodies against Ki-67 protein and proliferating cell nuclear antigen (PCNA). Cell Tissue Res. *283*, 191–201.

Wu, X., and Zhang, Y. (2017). TET-mediated active DNA demethylation: mechanism, function and beyond. Nat. Rev. Genet. *18*, 517–534.

Wu, X., Li, G., and Xie, R. (2018). Decoding the role of TET family dioxygenases in lineage specification. Epigenetics Chromatin *11*, 58.

Xiao, F.H., Wang, H.T., and Kong, Q.P. (2019). Dynamic DNA methylation during aging: a "prophet" of age-related outcomes. Front. Genet. *10*, 107.

Xie, C., Mao, X., Huang, J., Ding, Y., Wu, J., Dong, S., Kong, L., Gao, G., Li, C.Y., and Wei, L. (2011). KOBAS 2.0: a web server for annotation and identification of enriched pathways and diseases. Nucleic Acids Res. *39*, W316–W322.

Yamaguchi, S., Hong, K., Liu, R., Shen, L., Inoue, A., Diep, D., Zhang, K., and Zhang, Y. (2012). Tet1 controls meiosis by regulating meiotic gene expression. Nature *492*, 443–447.

Yang, J., Guo, R.P., Wang, H., Ye, X.Y., Zhou, Z.C., Dan, J.M., Wang, H.Y., Gong, P., Deng, W., Yin, Y., et al. (2016). Tet enzymes regulate telomere maintenance and chromosomal stability of mouse ESCs. Cell Rep. *15*, 1809–1821.

Yuan, L., Liu, J.G., Zhao, J., Brundell, E., Daneholt, B., and Hoog, C. (2000). The murine SCP3 gene is required for synaptonemal complex assembly, chromosome synapsis, and male fertility. Mol. Cell *5*, 73–83.

Yue, F., Cheng, Y., Breschi, A., Vierstra, J., Wu, W., Ryba, T., Sandstrom, R., Ma, Z., Davis, C., Pope, B.D., et al. (2014). A comparative encyclopedia of DNA elements in the mouse genome. Nature *515*, 355–364.

Zhang, R.R., Cui, Q.Y., Murai, K., Lim, Y.C., Smith, Z.D., Jin, S., Ye, P., Rosa, L., Lee, Y.K., Wu, H.P., et al. (2013). Tet1 regulates adult hippocampal neurogenesis and cognition. Cell Stem Cell *13*, 237–245.

Zhang, Q., Gao, M., Zhang, Y., Song, Y., Cheng, H., and Zhou, R. (2016). The germline-enriched Ppp1r36 promotes autophagy. Sci. Rep. *6*, 24609.

Zhou, W., Shao, H., Zhang, D., Dong, J., Cheng, W., Wang, L., Teng, Y., and Yu, Z. (2015). PTEN signaling is required for the maintenance of spermatogonial stem cells in mouse, by regulating the expressions of PLZF and UTF1. Cell Biosci. *5*, 42.

iScience, Volume *23*

Supplemental Information

Tet1 Deficiency Leads to Premature Reproductive Aging by Reducing Spermatogonia Stem Cells and Germ Cell Differentiation

Guian Huang, Linlin Liu, Huasong Wang, Mo Gou, Peng Gong, Chenglei Tian, Wei Deng, Jiao Yang, Tian-Tian Zhou, Guo-Liang Xu, and Lin Liu

Supplemental Information

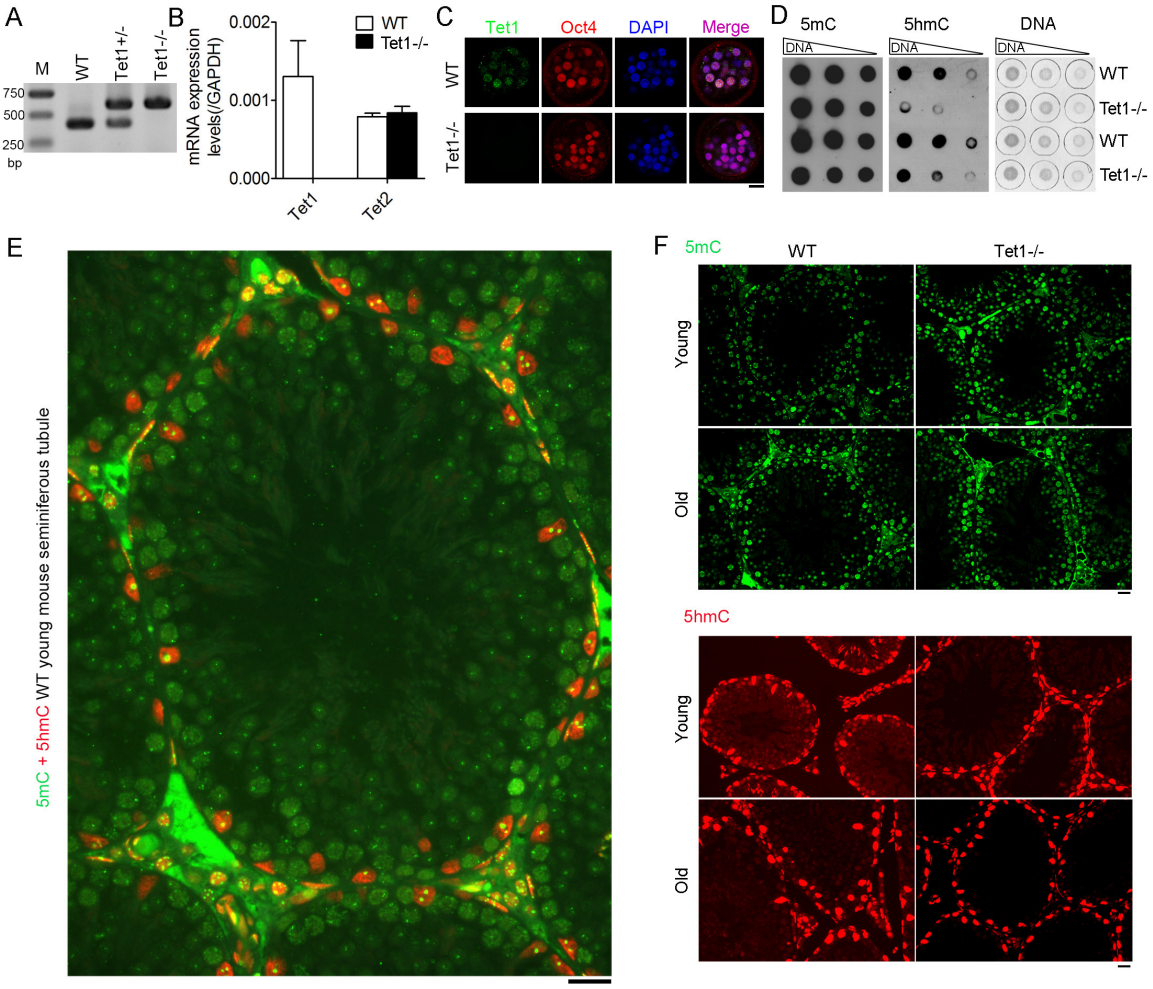

Figure S1. Genotyping of *Tet1* knockout (*Tet1*$^{-/-}$) mice and assay of 5mC and 5hmC, Related to Figure 1.

(A) Genotyping by PCR of mutant mice. Primer sequences are listed in Table S1. M, Marker. WT, wild-type.

(B) Relative expression levels by qPCR of *Tet1* and *Tet2* in WT and *Tet1*$^{-/-}$ testis. Primer sequences are listed in Table S1.

(C) Immunofluorescence microscopy of morula embryos confirming the protein expression of Tet1 in WT, but not in *Tet1*$^{-/-}$ embryos. Scale bar, 10 μm.

(D) Dot blot analysis of the genomic 5mC and 5hmC levels in the testis of WT and *Tet1*$^{-/-}$ mice.

(E) Representative images displaying immunofluorescence of 5mC and 5hmC in seminiferous tubules of young (3 month-old) mouse testis. Scale bar, 20 μm.

(F) Comparison of immunofluorescence of 5mC and 5hmC in seminiferous tubules of young (3 month-old) and old (11 month-old) WT and *Tet1*$^{-/-}$ mouse testes. Anti-5mC (mouse, Millipore, NA81, green), anti-5hmC (rabbit, Active-Motif, 39770, red). Scale bar, 20 μm.

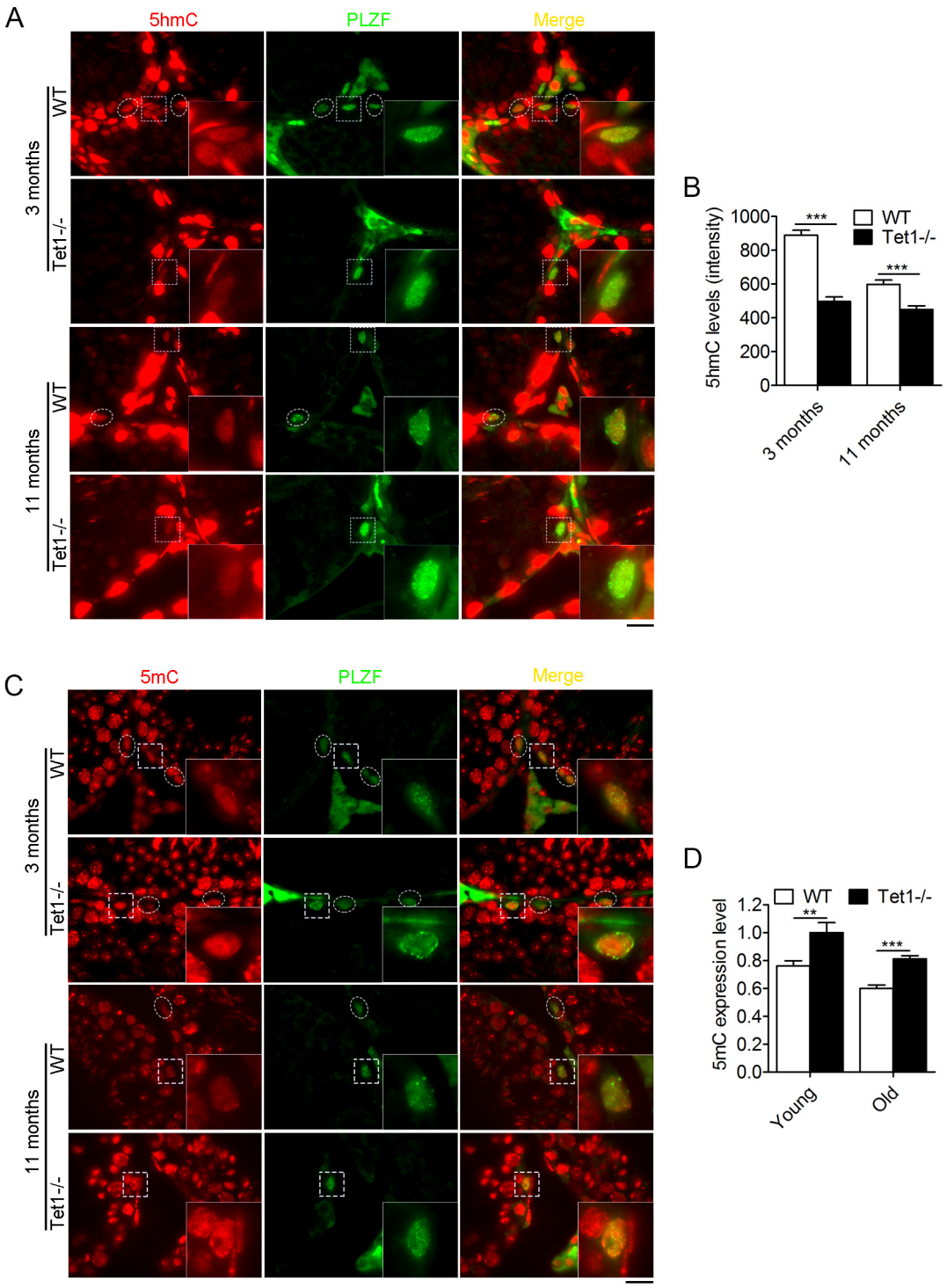

Figure S2. Co-Immunofluorescence of 5hmC or 5mC with PLZF on testis sections of *Tet1*$^{-/-}$ mice, Related to Figures 1 and 2.

(A) Representative images of spermatogonial stem cells (SSCs) co-stained with 5hmC (red) and PLZF (green) of the testis section from young (3 months) and old (11 months) male mice. Scale bar, 10 μm.

(B) Quantification of 5hmC intensity/levels in spermatogonia by ImageJ. More than 40 spermatogonia were randomly counted for each group in two repeated experiments. Data are represented as mean ± SEM. ***P < 0.001, Student's t-test.
(C) Representative images of SSCs co-stained with 5mC (red) and PLZF (green) of the testis section from young (about 3 months) and old (about 11 months) male mice. Scale bar, 10 μm.
(D) Quantification of 5mC intensity/levels in spermatogonia by ImageJ. More than 40 spermatogonia cells were randomly counted for each group in two repeated experiments. Data are represented as mean ± SEM. **p<0.01, ***P < 0.001, Student's t-test.
Anti-5mC (rabbit, Abcam, ab214727, red) and anti-5hmC (rabbit, Active-Motif, 39769, red) were used.

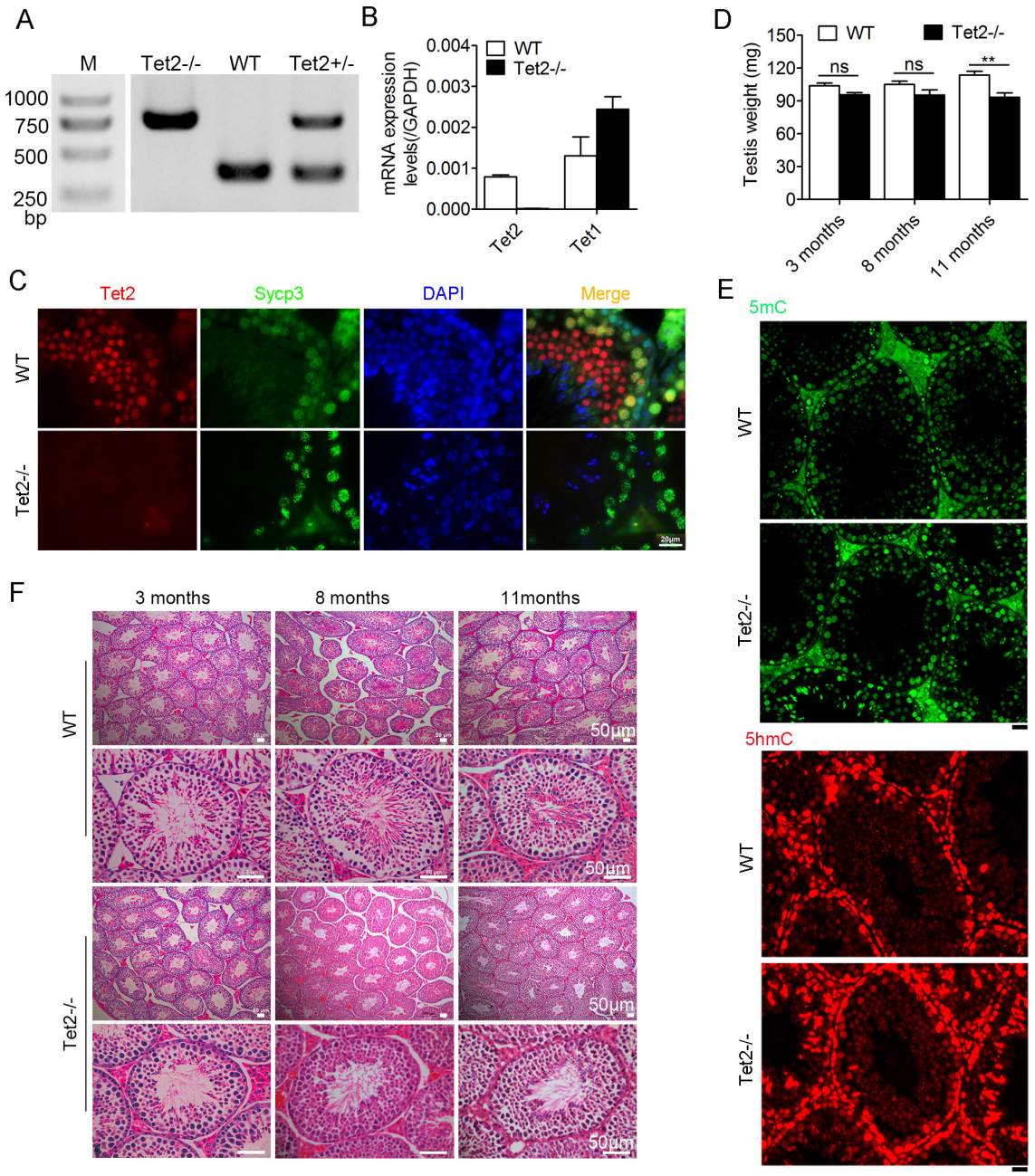

Figure S3. *Tet2* deficiency does not affect male fertility, Related to Figure 1.

(A) Genotyping by PCR of mutant mice. Primer sequences are listed in Table S1. M, Marker.

(B) Relative expression levels by qPCR of *Tet1* and *Tet2* in wild-type (WT) and *Tet2* KO (*Tet2*$^{-/-}$) testis. Primer sequences are listed in Table S1.

(C) Immunostaining of Tet2 and Sycp3 in the section of testis of *Tet2*$^{-/-}$ mice compared with WT mice. Scale bar, 20 μm.

(D) Average testis weight. n=4 mice for each group. Data are represented as mean ± SD. **p<0.01, ns, not significant (P>0.05). Student's t-test.

(E) Comparison of immunofluorescence of 5mC and 5hmC in seminiferous tubules of young (about 3 months) WT and *Tet2*$^{-/-}$ mouse testis. Anti-5mC (mouse, Millipore, NA81, green),

anti-5hmC (rabbit, Active-Motif, 39769, red). Scale bar, 20 μm.
(F) H&E-staining of the cross sections of seminiferous tubules from 3- 8- and 11-month-old WT and *Tet2*$^{-/-}$ mice. Scale bar, 50 μm.

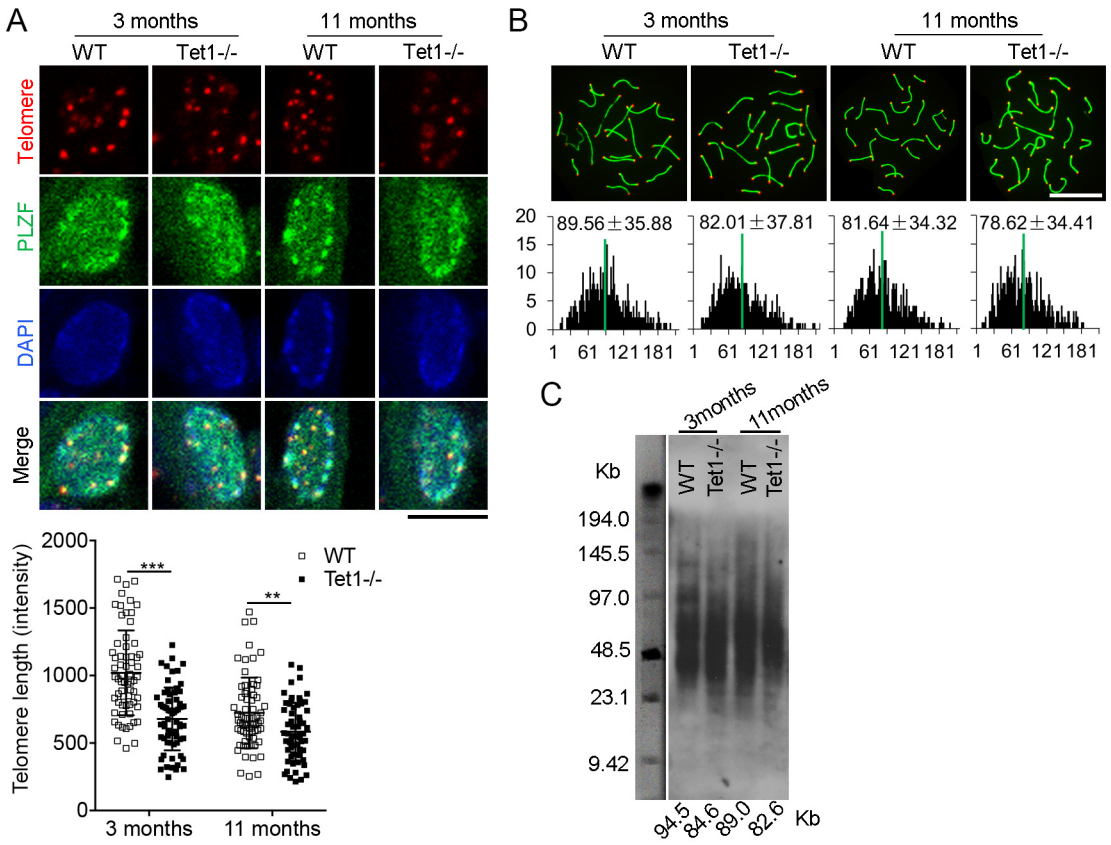

Figure S4. *Tet1* deficiency leads to telomere shortening, Related to Figures 1-3.

(A) Immunofluorescence-FISH images of telomeres (red) and PLZF (green). About telomeres of 60 spermatogonia shown by PLZF from 2-3 mice were quantified for each group. Data are represented as mean ± SD. **p<0.01, ***p < 0.001, ns, not significant (P>0.05). Student's t-test. Scale bar, 5 μm.

(B) Telomere-FISH (red) and immunofluorescence of Sycp3 (green) of pachytene spermatocyte spreads and histogram showing distribution of relative telomere length as TFU by Q-FISH. The medium telomere length (green bars) is shown as mean ± SD. About 20 chromosome spreads from 2-3 mice were quantified for each group. Scale bar, 20 μm.

(C) Telomere length distribution shown as TRF by Southern blot analysis. Repeat, 2-3 mice.

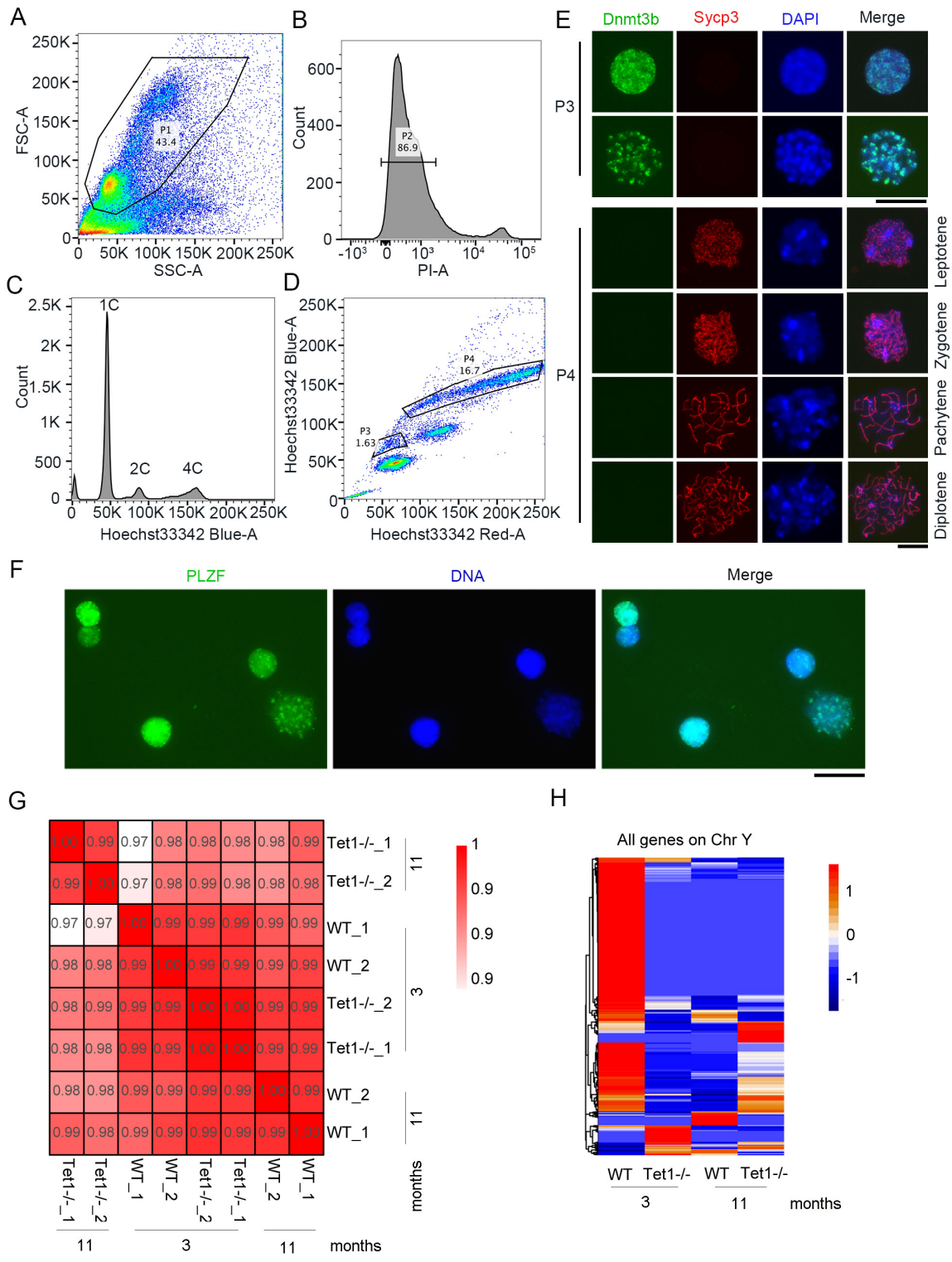

Figure S5. Gating strategies for isolating spermatogonia populations from testicular cell suspension, Related to Figure 4.

(A) Cell debris exclusion based on low light scattering. FSC and SSC represent two different laser beams within flow cytometry that can detect cell size and cell adherence respectively.

Small FSC value indicates cell debris, whereas large SSC values indicates adherent cells.
(B) Dead cell exclusion based on propidium iodide (PI) fluorescence. PI indicates dead cells. P2 represents live cells.
(C) DNA content exclusion based on Hoechst-blue fluorescence.
(D) Gating on individual testicular populations based on Hoechst-blue/Hoechst-red fluorescence. P2 cell populations belong to P1 populations. P3 and P4 populations belong to P2 cell populations. P3 cell populations mostly containing spermatogonia were used for RNA-seq.
(E) Immunofluorescence characterization of spermatogonia (Spg) and primary spermatocytes. Cells were stained with antibodies specific for Dnmt3b (green) and Sycp3 (red). Scale bar, 20 μm.
(F) Immunofluorescence of P3 cell populations following cell sorting, showing existence of both spermatogonia PLZF (compact small nuclei, green) and spermatocytes with de-condensed nuclei. Scale bar, 20 μm.
(G) Pearson's correlation coefficient graph analysis of 3 months WT and *Tet1*$^{-/-}$, and 11 months WT and *Tet1*$^{-/-}$ mice. The value of 1.0 represents total positive correlation and 0 represents no correlation between the two samples.
(H) Pheatmap illustrating all genes on Chromosome Y.

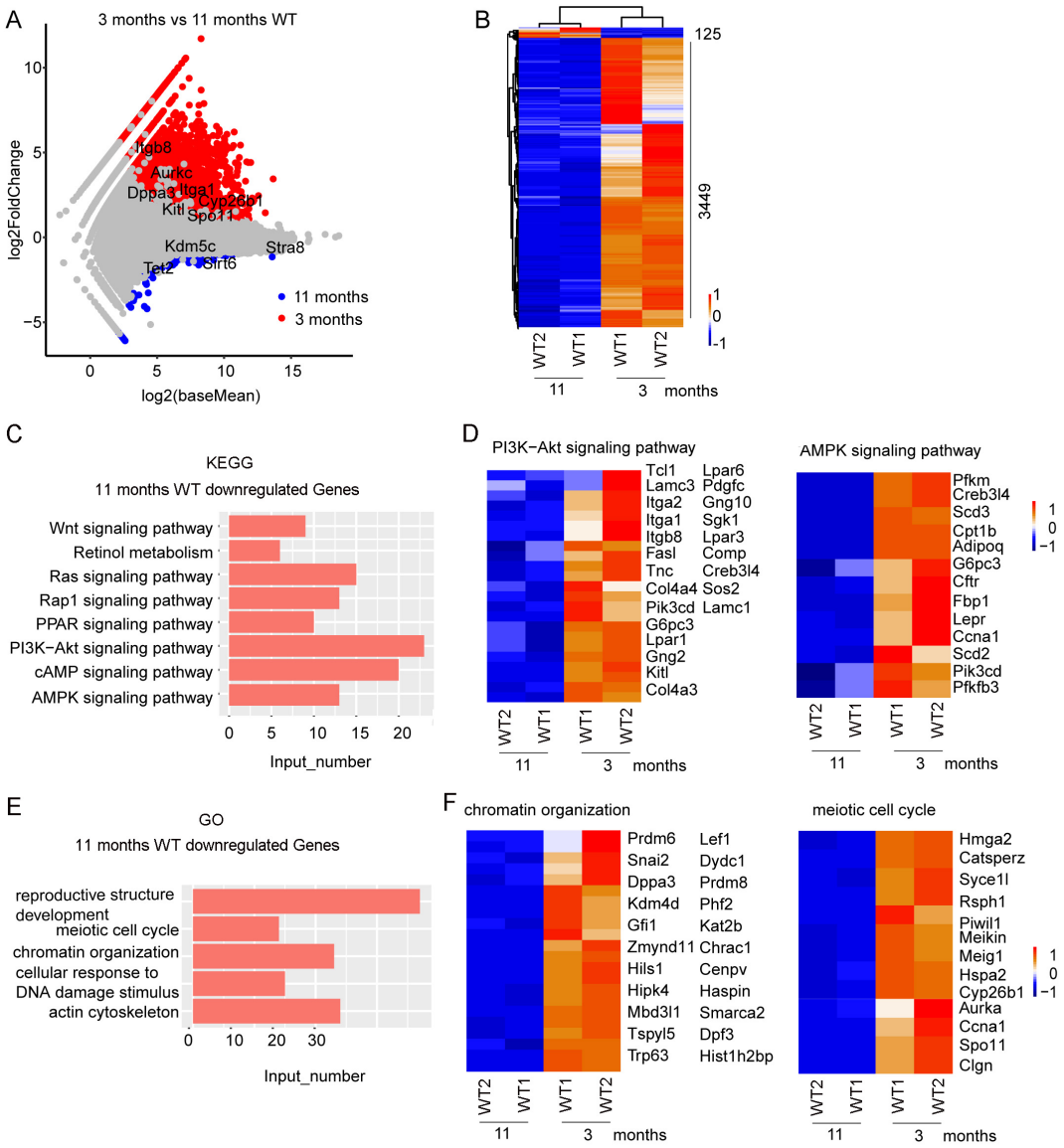

Figure S6. Effects of age on transcriptome of spermatogonia cells, Related to Figures 4 and 5.

(A) Scatter plot showing gene expression between 3 and 11 month-old WT mouse spermatogonia. Red represents genes with higher expression levels in 3 months WT, and blue represents genes with higher expression levels in 11 months WT, grey represents no significance between 3 and 11 months WT spermatogonia.

(B) Differential gene expression shown by pheatmap. Differential genes were selected by the standard of log2Foldchange>1, and p value<0.05.

(C) KEGG results enriched by the downregulated genes of 11 months WT spermatogonia by KOBAS websites (http://kobas.cbi.pku.edu.cn/index.php).

(D) Pheatmap showing the results of genes enriched in PI3K-Akt signaling pathway and AMPK signaling pathway.

(E) GO results enriched by the downregulated genes of 11 months WT by KOBAS websites.

(F) Pheatmap showing the results of genes enriched in chromatin organization and meiotic cell cycle.

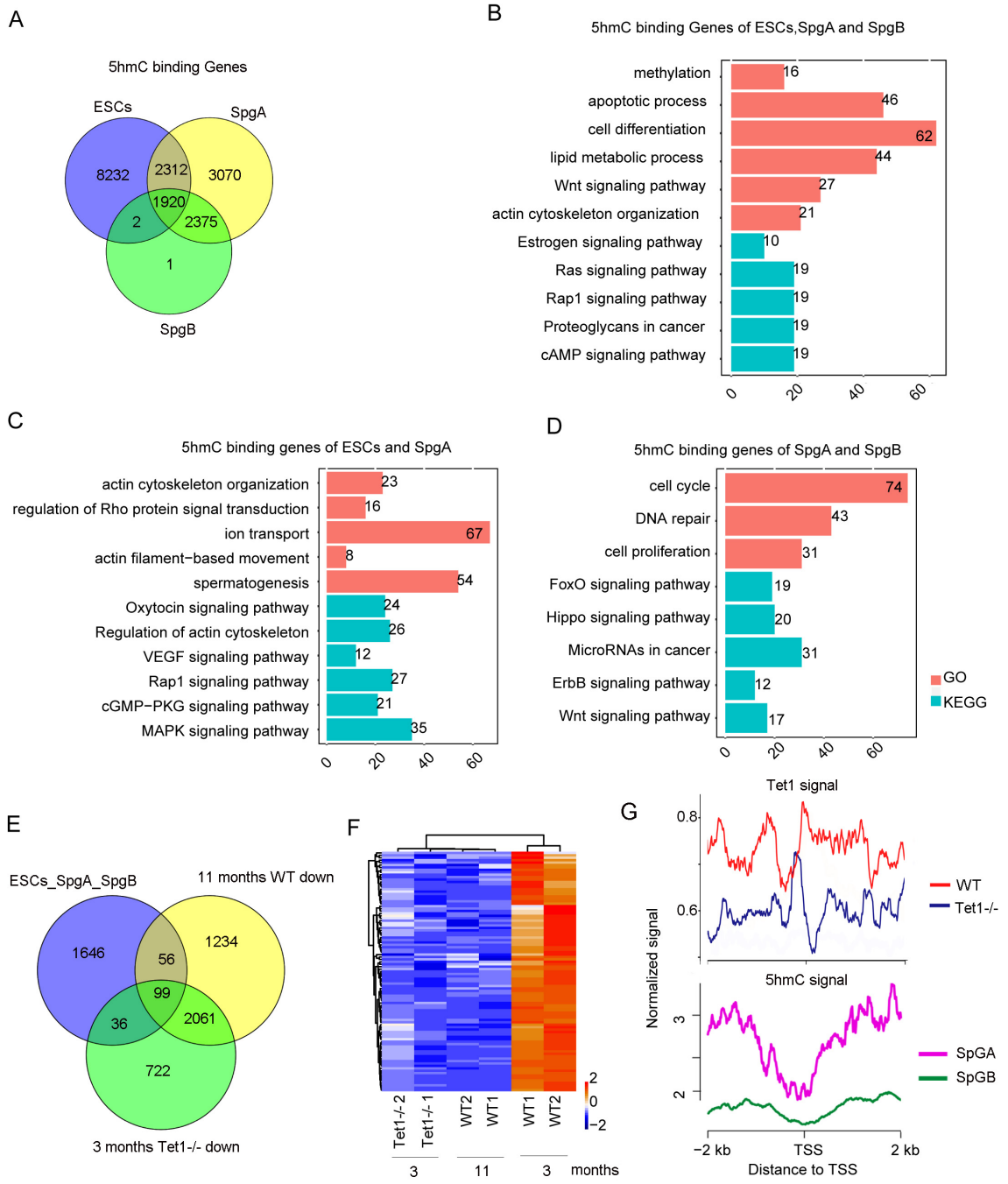

Figure S7. 5hmC and Tet1 binding genes in spermatogonia cells and ESCs, Related to Figures 6 and 7.

(A) Venn diagram of 5hmC binding genes in ESCs (Williams et al., 2011), type A and type B spermatogonia cells (Gan et al., 2013).

(B) GO and KEGG results of 1,920 genes overlapped in Figure (A). GO results showed that these genes were enriched in methylation, apoptotic process, cell differentiation. KEGG results showed that these genes were enriched in estrogen signaling, Ras, Rap1

signaling, and cAMP signaling pathway. Red represents GO enrichment results, and blue represents KEGG results.
(C) GO and KEGG results of 2,312 genes overlapped in Figure (A). GO results showed that these genes were enriched in actin cytoskeleton organization, regulation of Rho protein signal transduction, ion transport, actin filament-based movement and spermatogenesis. KEGG results showed that these genes were enriched in Oxytocin signaling, VEGF signaling, Rap1 signaling, cGMP-PKG signaling and MAPK signaling pathway. Red represents GO enrichment results, and blue represents KEGG results.
(D) GO and KEGG results of 2,375 genes overlapped in Figure (A). GO results showed that these genes were enriched in cell cycle, DNA repair, cell proliferation. KEGG results showed that these genes were enriched in Foxo signaling, Hippo signaling, Wnt signaling. Red represents GO enrichment results, and blue represents KEGG results.
(E) Venn diagram showing overlapped genes in Figure (A) that were downregulated in 3 months *Tet1*$^{-/-}$ and 11 months WT males. There were 99 genes overlapped among the groups.
(F) Pheatmap showing the 99 genes downregulated in the 3 months *Tet1*$^{-/-}$ and 11 months WT males, compared with 3 months WT males.
(G) Normalized signal of 5hmC or Tet1 by ChIP-seq on the 99 genes in Spermatogonia A and B type cells, and 3 month-old WT and *Tet1*$^{-/-}$ spermatogonia cells.

Table S1 Primers for genotyping and quantitative realtime PCR, Related to Figures S1 and S3.

Genotyping	Tet1C	CAGTAGTATTTTGCCTGCCTGCAT
	Tet1F	CATCCTAAATAACCCAACCACCAA
	Tet1R	TTCCCTAAGGAGTTTACTGCAACG
	Tet2-Gf1	AGTTCACCCTTCTCATGTGGATACT
	Tet2-Gr1	CTCTTTACCATACTTGATTGGCTCT
	Tet2-Gr4-6	AGTCCTTGGTCATCAGGAACTCTA
qPCR	Tet1RT-F1	CCTCACAGGCACAGGTTACA
	Tet1RT-R1	ATTTGGGGCCATTTACTGGT
	Tet2RT-F	TGTTGTTGTCAGGGTGAGAATC
	Tet2RT-R	TCTTGCTTCTGGCAAACTTACA

Transparent Methods

Mice and care

Tet1 and *Tet2*-deficient mice, generated from Guoliang Xu lab (Shanghai Institutes for Biological Sciences, Chinese Academy of Sciences, Shanghai 200031, China)(Zhang et al., 2013), were housed and cared for in a pathogen-free facility at Nankai University. All animal experiments were approved by the Institutional Animal Care and Use Committee at Nankai University. All animal studies were carried out in strict accordance with the recommendations in the Guide for the Care and Use of Laboratory Animals of Nankai University. All efforts were made to minimize the number of animals used by the experimental design. Heterozygous mice were interbred to obtain *Tet1*-or *Tet2*--knockout ($Tet1^{-/-}$, $Tet2^{-/-}$) mice. The pups were genotyped by PCR using specific genotype primers listed in Table S1.

qPCR

Testis mRNA was directly reverse transcribed to cDNA by M-MLV Reverse transcriptase (639524, Clontech). Real-time qPCR reaction was performed using FastStart Universal SYBR Green Master (4913914001, Roche). All genes were confirmed for their specificity by dissociation curves and amplification curves, and *Gapdh* served as housekeeping gene for normalization of gene expression.

Tissue collection and histology

Testes were collected from 3 months, 8 months and 11months mice by 4% PFA fixation at 4°C overnight, dehydrated in an ethanol series, and embedded in paraffin wax. Sections in 5μm were cut, following deparaffinization and rehydration, then stained with hematoxylin and eosin Y (H&E) for histological analysis.

TUNEL assay

Apoptosis assay for sections was performed by TUNEL staining following DeadEnd™ Fluorometric TUNEL System (G3250; Promega). Apoptotic cell number

per tubule was calculated by dividing the total number of TUNEL-positive germ cells by the total number of seminiferous tubules examined for each mouse.

Dot blot

For dot blot, DNA were denatured at 99°C for 5 min then spotted onto nylon membranes (RPN2020B; GE Healthcare). After UV cross-linking membranes were blocked 30min with 5% non-fat milk in PBS-T, then incubated for one hour with 5mC or 5hmC antibodies at room temperature, 30 min with HRP conjugated donkey anti-Rabbit IgG (NA934V; GE Healthcare), and visualized using the Immobilon Western HRP Substrate (WBKLS0500; Millipore).

Spermatocyte chromosome spreading

Chromosome spreading was performed using the drying-down technique described in Peters et al. (Peters et al., 1997). Seminiferous tubules were placed in a hypotonic extraction buffer containing 30 mM Tris, 50 mM sucrose, 17 mM trisodium citrate dihydrate, 5 mM EDTA, 0.5 mM DTT and 0.5 mM phenylmethylsulphonyl fluoride (PMSF), pH 8.2 for 30min, then torn to pieces in 100 mM sucrose (pH 8.2) using syringe needles to make a cell suspension. The cell suspension was placed on slides just dipped into 1% paraformaldehyde (pH9.2) containing 0.15% Triton X-100. Nuclei were dried for at least 2h at room temperature. The slides were then washed for 2 min in 0.4% Photoflo (Kodak) and dried at room temperature, finally, stored at -20 °C.

Immunofluorescence microscopy

For tissue section immunofluorescence, following deparaffinization, rehydration, sections were boiled for 3min at 120°C in 0.01% sodium citrate buffer (pH 6.0) for antigen retrieval, permeabilized in 0.2% TritonX-100 for 30 min, blocked with 5% goat serum and 0.1% BSA for 2h, then incubated with primary antibodies at 4°C overnight. After washing with PBS for three times, sections were incubated with appropriate secondary antibody (Alexa Fluor 594 or 488, Invitrogen) for 2h at room temperature. Immunostaining of spermatocytes performed as described in Liu et al.

(Liu et al., 2004). Slides were washed for 10 min in PBS, blocked in ADB buffer (2% goat serum, 3%BSA in PBS containing 0.1% TritonX-100) for 1h, incubated with primary antibodies at 4°C overnight, then secondary antibodies for 1h at room temperature. After washing, the slides were mounted in Vectashield (Vector Laboratories) containing 1μg/mL DAPI. Images were collected using a Zeiss Axio Imager Z2 (Carl Zeiss). The following primary antibodies were used for immunofluorescence: DAZL (ab34139; Abcam), Sycp3 (NB 300-232; Novus Biologicals), PCNA (SC25280; Santa Cruz), Sycp3 (ab97672; Abcam), PLZF(sc-28319; Santa Cruz), γH2AX (05–636; Millipore), MLH1 (550838; BD Pharmingen), 5hmC(39769; Active motif), 5mC(NA81; Millipore), 5mC(ab214727; Abcm), or Rad51 (ab88572; Abcam).

Telomere quantitative immunofluorescence in situ hybridization (IF-FISH)

Telomere length was estimated by IF-FISH. IF-FISH was performed on spermatocyte spread and tissue section. The immunofluorescence was performed as described above. After secondary antibody incubation, the spread was fixed in 4% PFA for 15min, washed with PBS, dehydrated in an ethanol series, then dried. Telomeres were denatured at 80°C for 3 min and hybridized with FITC-labeled (CCCTAA) peptide nucleic acid (PNA) probe (F1009; Panagene) at 0.5μg/ml. For quantitative measurement of telomere length, telomere fluorescence intensity was integrated using the TFL-TELO program (a gift kindly provided by P. Lansdorp, Terry Fox Laboratory).

TRF by Southern blot analysis

The average terminal restriction fragments (TRF) length was determined according to the commercial kit (TeloTAGGG Telomere Length Assay, 12209136001; Roche Life Science). DNA was extracted by traditional phenol:chloroform:isoamyl alcohol method. 3μg DNA was digested with MboI (NEB) for 15 h and the DNA fragments separated by 1% agarose gel for 16 h at 6V/cm in 0.5 × TBE buffer using CHEF DR-III pulse-field system (Bio-Rad). Gels were denatured, neutralized, and

transferred to nylon membrane (RPN2020B; GE Healthcare) for 24 h. The membrane was hybridized with digoxigenin (DIG)-labeled telomere probe at 42°C overnight and incubated with anti-DIG-alkaline phosphatase antibody. Telomere signal was detected by chemiluminescence after adding substrate solution on membrane.

Spermatogonia purification

Testes were collected from 3 month and 11 month-old mouse and dissociated by double enzymes digestion method as described with slight modification (Gaysinskaya et al., 2014). Briefly, testes were decapsulated and digested in PBS containing 1mg/mL Collagenase Type IV (#17104-019; Gicbo) and 5U/mL DNase I (#4536282001; Roche) for 15min at 33°C. After washing with PBS to exclude interstitial testicular cells, tubules were digested in Trypsin-EDTA solution at 33□ for total 15min. Cells were filtered through a 40 μm nylon cell strainer. After a PBS wash, cells were resuspended in PBS and stained with Hoechst33342 (5 μg/10^6 cells) at 33□ for 30 min, then stained with 2 μg/mL Propidium Iodide (PI, #P4864; Sigma-Aldrich) before sorting. Analyses and cell sorting were performed on BD Aria III flow cytometer. The dead cells were excluded based on PI fluorescence. The Hoechst33342 was excited using 355 nm laser and detected in two distinct channels: the Hoechst Blue (450 band-pass filter) and the Hoechst Red (670 nm long pass filter). The spermatogonia and primary spermatocytes were sorted and identified by immunofluorescence. Cells were collected for RNAseq.

Cell isolation and lysis

RNA-seq libraries were prepared using Smart-seq2 methods described in Picelli et al. (Picelli et al., 2014). 1000 cells per sample were resuspended in PBS added with 0.1% BSA (A3311-10g, Sigma) and transferred to the bottom of a PCR tube (8-strip, nuclease-free, thin-walled PCR tubes with caps, PCR-0208-C, Axygen) containing 3 μl lysis buffer composed of with oligo (dT) primer, 0.02% Triton X-100, and 2U/μl Recombinant RNase Inhibitor (RRI, 2313A, Takara). Samples were frozen in liquid

nitrogen and stored at -80°C or reversed immediately on ice to prevent RNA degradation.

Reverse transcription

One μl deoxy-ribonucleoside triphosphate (R0191,Thermo Scientific) was added to the melt frozen or fresh samples in tubes on ice and vortexed gently, and incubated at 37°C for 3 min. The cDNAs were then synthesized by template switch oligo (TSO) primer and reverse transcription primer, and SuperScript™ II Reverse Transcriptase (18064071,Thermo Scientific) followed by 15 cycles of PCR using KAPA HotStart ReadyMix (KK2602, KAPA Biosystems) and then purified using Agencount AMPure XP beads (A63881, BECKMAN).

Library construction and sequencing

The libraries were prepared by using TruePrep DNA Library Prep Kit V2 for Illumina® (TD503-02, Vazyme Biotech) according to the manual instruction. Samples were barcoded and multiplex sequenced with a 150 bp paired-end sequencing strategy on Illumina Hiseq x10.

Processing RNA-seq data

RNA-seq raw reads were trimmed to remove adaptor contaminants and low-quality bases using Trimmomatic (version 0.36) with defined parameters and low-quality bases (Bolger et al., 2014). The clean reads were aligned to mouse genome (mm10, UCSC version) using Hisat2 (version2.1.0) (Kim et al., 2015), with default parameters, and uniquely mapped reads were counted with Featurecounts (version 1.6.4) (Liao et al., 2014). In light of the difference in sequencing length between samples, we quantified gene expression levels with transcripts per kilobase of exon model per million mapped reads (TPM), data visualization and PCA/clustering analysis, using the PCA int () function in R and the first two principal components of variance.

Identification of differentially expressed genes

Dynamic changes of differentially expressed genes (DEGs) between different groups were analyzed using Deseq2 (Love et al., 2014). DEGs were defined only if pvalue was < 0.05, and a fold change (log2-transferred) was >1. GO analysis was performed on KOBAS websites (Xie et al., 2011). Gene expression were shown using pheatmap and ggviolin, by R package Pheatmap, ggplot2 and ggpubr. All spermatogenesis-associated GO term gene sets were collected from MGI.

Tet1 ULI-NChIP-seq

For ULI-NChIP-seq (Brind'Amour et al., 2015), 50,000 cells separated by FACS were used per reaction. Cells in Nuclei Extraction Buffer was fragmented depending on input size chromatin for 5–7.5 min using MNase at 21 or 37 °C. Chromatin was pre-cleared with 5 µl of 1:1 protein A:protein G Dynabeads (Life Technologies) and with 1 mg of Tet1 (1749-1902, Cat# Company or custom-made)–bead complexes overnight at 4 °C. Chip-DNA was purified by phenol chloroform, ethanol-precipitated and Chip-DNA was re-suspended in 10 mM Tris-HCl pH 8.0. The sequence libraries were generated using ATseq for the Illumina platform (0001), following the manufacturer's instructions. Paired-end 150 sequencing was performed on a HiSeq X10 (Illumina).

Processing ChIP-seq data and DNA methylation

The data on GEO database are used, including ChIP-data, H3K4me3 (GSM1202705) (Hammoud et al., 2014), Tet1-C_shTet1 (GSM611193), and Tet1-Ctrl (GSM611194) (Williams et al., 2011), 5hmC data in spermatogonia cells (GSE35005)(Gan et al., 2013), Tet1(GSM611199) and shTet1(GSM611201) of ESCs (Williams et al., 2011), 5mC data, Tet1-Ctrl (GSM611203) and shTet1(GSM611205) in ESCs (Williams et al., 2011). These data were converted by SRA Toolkit to fq files and then all the reads were aligned to the mouse genome (mm10, UCSC version) using bowtie2 (Langmead and Salzberg, 2012)(version 2.2.3) with default parameters. We used command predicted in MACS2 (Liu, 2014; Zhang et al., 2008) (version 2.1.1) to

predict fragment size in all ChIP-seq samples and predicted peaks using command callpeak in MACS2 with defined parameters (-extsize 226, -q 0.05). We visualized genes with IGV software (Thorvaldsdottir et al., 2013).

Statistical analysis

The data presented are means ± SD of independent replicates (n ≥ 3) (major RNA-seq analysis was performed three times and two repeats are shown). Student's t test was applied for statistical analysis using GraphPad Prism 7 (GraphPad Software, San Diego, CA). Statistically significance was defined as $P < 0.05$ (*), $P<0.01$(**) or $P<0.001$(***).

References

Bolger, A.M., Lohse, M., and Usadel, B. (2014). Trimmomatic: a flexible trimmer for Illumina sequence data. Bioinformatics *30*, 2114-2120.

Brind'Amour, J., Liu, S., Hudson, M., Chen, C., Karimi, M.M., and Lorincz, M.C. (2015). An ultra-low-input native ChIP-seq protocol for genome-wide profiling of rare cell populations. Nat Commun *6*, 6033.

Gan, H., Wen, L., Liao, S., Lin, X., Ma, T., Liu, J., Song, C.X., Wang, M., He, C., Han, C*., et al.* (2013). Dynamics of 5-hydroxymethylcytosine during mouse spermatogenesis. Nat Commun *4*, 1995.

Gaysinskaya, V., Soh, I.Y., van der Heijden, G.W., and Bortvin, A. (2014). Optimized flow cytometry isolation of murine spermatocytes. Cytometry A *85*, 556-565.

Hammoud, S.S., Low, D.H., Yi, C., Carrell, D.T., Guccione, E., and Cairns, B.R. (2014). Chromatin and transcription transitions of mammalian adult germline stem cells and spermatogenesis. Cell Stem Cell *15*, 239-253.

Kim, D., Langmead, B., and Salzberg, S.L. (2015). HISAT: a fast spliced aligner with low memory requirements. Nat Methods *12*, 357-360.

Langmead, B., and Salzberg, S.L. (2012). Fast gapped-read alignment with Bowtie 2. Nat Methods *9*, 357-359.

Liao, Y., Smyth, G.K., and Shi, W. (2014). featureCounts: an efficient general purpose program for assigning sequence reads to genomic features. Bioinformatics *30*, 923-930.

Liu, L., Franco, S., Spyropoulos, B., Moens, P.B., Blasco, M.A., and Keefe, D.L. (2004). Irregular telomeres impair meiotic synapsis and recombination in mice. Proc Natl Acad Sci U S A *101*, 6496-6501.

Liu, T. (2014). Use model-based Analysis of ChIP-Seq (MACS) to analyze short

reads generated by sequencing protein-DNA interactions in embryonic stem cells. Methods Mol Biol *1150*, 81-95.

Love, M.I., Huber, W., and Anders, S. (2014). Moderated estimation of fold change and dispersion for RNA-seq data with DESeq2. Genome Biol *15*, 550.

Peters, A.H., Plug, A.W., van Vugt, M.J., and de Boer, P. (1997). A drying-down technique for the spreading of mammalian meiocytes from the male and female germline. Chromosome Res *5*, 66-68.

Picelli, S., Faridani, O.R., Bjorklund, A.K., Winberg, G., Sagasser, S., and Sandberg, R. (2014). Full-length RNA-seq from single cells using Smart-seq2. Nat Protoc *9*, 171-181.

Thorvaldsdottir, H., Robinson, J.T., and Mesirov, J.P. (2013). Integrative Genomics Viewer (IGV): high-performance genomics data visualization and exploration. Brief Bioinform *14*, 178-192.

Williams, K., Christensen, J., Pedersen, M.T., Johansen, J.V., Cloos, P.A., Rappsilber, J., and Helin, K. (2011). TET1 and hydroxymethylcytosine in transcription and DNA methylation fidelity. Nature *473*, 343-348.

Xie, C., Mao, X., Huang, J., Ding, Y., Wu, J., Dong, S., Kong, L., Gao, G., Li, C.Y., and Wei, L. (2011). KOBAS 2.0: a web server for annotation and identification of enriched pathways and diseases. Nucleic Acids Res *39*, W316-322.

Zhang, R.R., Cui, Q.Y., Murai, K., Lim, Y.C., Smith, Z.D., Jin, S., Ye, P., Rosa, L., Lee, Y.K., Wu, H.P.*, et al.* (2013). Tet1 regulates adult hippocampal neurogenesis and cognition. Cell Stem Cell *13*, 237-245.

Zhang, Y., Liu, T., Meyer, C.A., Eeckhoute, J., Johnson, D.S., Bernstein, B.E., Nusbaum, C., Myers, R.M., Brown, M., Li, W.*, et al.* (2008). Model-based analysis of ChIP-Seq (MACS). Genome Biol *9*, R137.